International Journal of Disaster Risk Reduction 114 (2024) 104929

Contents lists available at ScienceDirect

International Journal of Disaster Risk Reduction

journal homepage: www.elsevier.com/locate/ijdrr

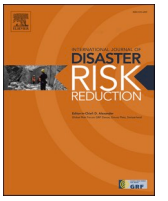

A multi-step framework for measuring post-earthquake recovery: Integrating essential infrastructure System's serviceability in building functionality

Ram Krishna Mazumder [a,b,*], Elaina J. Sutley [b]

[a] Arcadis U.S. Inc., Akron, OH 44308, USA
[b] Civil, Environmental and Architectural Engineering, University of Kansas, Lawrence, KS 66045, USA

A B S T R A C T

Measuring and predicting the functionality of buildings is a core aspect of community resilience analysis, which is jointly dependent on structural integrity and essential services provided by critical infrastructure systems. A functional building is one that is used for its intended services. This paper develops a multi-step community-level functionality analysis framework by modelling: (1) building functionality that integrates the building's structural performance, essential water and electric power service performance, and physical accessibility through road networks; (2) portfolio-level building recovery by aggregating functionality of buildings for an entire community; and (3) serviceability of infrastructure systems. Graph theory is applied to assess performance of infrastructure systems. The cascading effect of water pipe failure on the road network is modelled through geographic dependency analysis. Post-earthquake water demand changes due to household dislocation and return, and increased water service demand at essential facilities are captured to model the performance of the water network under stressed conditions. The framework also assesses household-level housing recovery and integrates results with physical damage repair to more holistically depict the functional recovery of buildings from the perspective that buildings must be occupied to be fully functional. The proposed framework is illustrated for a scenario earthquake for the virtual community of Centerville. Findings provide an up-to-date measurement of post-disaster functionality for buildings and critical infrastructure systems that can guide decision-makers during pre-disaster planning and post-disaster recovery. The example demonstrates that consideration of essential infrastructure services significantly alters the functionality of the built environment during the recovery process. For instance, power outages resulted in functionality loss of up to 75 % of physically operable buildings for as much as 14 days. Consideration of physical accessibility loss to nearest road segments resulted in a portfolio functionality drop of up to 9 % for 6 days, and partial water shortage significantly hampered the functionality of the impacted area, including the regional hospital. Approximately 3 % of households were unable to repair their damaged homes and became homeless. The proposed framework enables risk-informed decisions regarding long-term recovery at the community scale with inclusion of those living at the margins and most susceptible to long-term negative consequences from disasters.

1. Introduction

Functionality of a system is defined as the system's ability to perform its intended functions. For a community, functionality thus includes providing shelter, healthcare, employment, education, and social and cultural networks and opportunities. Built system is the cornerstone of a functioning community through providing the buildings required for sheltering, for accessing healthcare, education and employment, and for hosting events that bring people together, as well as through providing the essential utility services, such as power, water, wastewater, and telecommunications, that make buildings themselves function. The interdependent and temporal process of functionality recovery of built system from extreme events remains a poorly understood topic, and research on analyzing the

* Corresponding author. Arcadis U.S. Inc., Akron, OH 44308, USA.
E-mail addresses: ramkrishna.mazumder@arcadis.com, rxm562@case.edu (R.K. Mazumder), enjsutley@ku.edu (E.J. Sutley).

https://doi.org/10.1016/j.ijdrr.2024.104929
Received 22 March 2024; Received in revised form 20 October 2024; Accepted 24 October 2024
Available online 30 October 2024

functionality of a community is rare. Buildings and infrastructure systems are interdependent where infrastructure systems can be regarded as the physical structure of a community, such as roads, water and wastewater systems, bridges, and energy systems, etc., that supports wellbeing and smooth functionality of the buildings and society (Mazumder et al., 2018; ASCE, 2021). Over the last decade, resilience was studied for individual infrastructure system, such as Water Distribution System (WDS) [1–4], Electrical Power Network (EPN) [5–7], Transportation Network (TN) [8–11], Wastewater Collection System [12,13], and Gas Transportation Network [14,15], as well as for buildings in general [16–18]. Since the failure of one infrastructure system often leads to the failure of other infrastructure systems, some studies have analyzed cascading impact and interdependency among more than one infrastructure systems [19–21] but were largely limited by not capturing the interaction between buildings, utility services, and especially occupancy or use.

Many recent studies have attempted to analyze community resilience comprehensively, which account for the interaction between buildings and infrastructure systems ([22–29]; Han and Koliou 2023; [30,31]). Although these community resilience studies (e.g., Ref. [23,24]) did consider the interaction between buildings and infrastructure systems, their analysis did not account for building functionality holistically, such as building's physical access to the road network or occupancy status. Another drawback is that these studies overlooked how the social characteristics of households can affect the recovery process. Furthermore, post-disaster demand changes (i.e., due to population dislocation or relocation) on damaged infrastructure systems is not accounted for in existing functionality models, which is crucial to account for the flow analysis of network systems during the restoration process. The present research fills this gap by developing a comprehensive framework for estimating post-earthquake community functionality by modelling building functionality restoration and integrating utility services, physical damage and repair while accounting for realistic demand changes due to physical damage and population dislocation in WDS serviceability analysis, building's physical access to the road network, system interdependency, social characteristics in household level housing recovery.

2. Literature review

2.1. Building functionality and recovery

Although buildings rely on other systems to be functional, building design codes focus on preserving occupant safety and do not specify requirements for reducing functionality loss caused by design-level or extreme loads that lead to service disruptions. Recent disasters have shown that service disruption can lead to building occupant fatality, especially for the most vulnerable populations, including those who rely on power-dependent medicines and medical devices [32,33]. To resume normal activities and access to emergency and essential services (e.g., hospital, grocery) after a disaster, road network accessibility to buildings is crucial [34,35]. Furthermore, service disruptions, including lost accessibility through the transportation network, can cause organizations and businesses to close – either temporarily or permanently – with many indirect consequences, including work disruption for employees, decreased service offerings to the community, and local economic decline, which all impact community-level functionality and recovery [29,35–37].

Researchers have evaluated the functionality of buildings using various proxies, such as structural and nonstructural performance, repair time, re-occupancy time, housing recovery, and utility service restoration, etc. [35,38–41], where many of these were left as qualitative relationships or quantified with limited empirical data or major simplifying assumptions. Almufti and Willford [42] presented post-earthquake downtime assessment methodology where various functionality recovery of buildings (i.e., re-occupancy, functional and full recovery) are defined based on building repair time estimated through FEMA P-58 probabilistic seismic performance assessment tool and utility disruption. Recent studies (e.g., Ref. [25–27]) applied probabilistic framework for damage assessment and put an effort in detailing structural damage levels. Terzic et al. [25] developed a generic fault tree method where various structural components and utilities (e.g. HVAC, Electrical, Plumbing) are equally weighted in estimating functionality of buildings. Cook et al. [26] also applied FEMA P-58 approach and used fault tree model to connect component-level damage to structural system performance. Molina Hutt et al. (2022) analyzed how tall building design relates to functionality recovery to characterize performance goals for re-occupancy and recovery, particularly for tall buildings. In addition to utilizing the existing FEMA P-58 to estimate repair cost and REDi approach to model temporal building recovery, the authors accounted for delays in repair initiation, labor allocation, and repair sequencing. Mohammadgholibeyki et al. [43,44]; evaluated feasibility of functionality achievement of retrofitted reinforce concrete buildings depending on various strategies and motivation. Other researchers (e.g., Ref. [45]) measured important building's (i.e., hospital) functionality based on the amount of useable physical space.

Comparably fewer models have attempted to determine the holistic functionality of buildings considering the coupled interaction between buildings and essential infrastructure services. Recent studies [17,23–26,29,46] developed simulation-based techniques that linked building physical performance with essential utility services. Aghababaei and Koliou [29,37] and Han and Koliou (2023) used agent-based model where various physical systems (e.g. water network) are modelled as an agent and logical flows of interrelationship among these agents are accounted for resilience and mitigation strategy simulation at the community level. While many components are blend, a large amount of assumption may limit (e.g. coupled performance of interdependent components) its application. Blagojević et al. [30] provided a computational framework to connect individual building-level recovery to regional-scale recovery, accounted for various factors associated with building recovery and regional resource constrains. Although these studies made significant progress in defining the functionality of buildings, these models did not incorporate physical access to the road network. Moreover, most of the past studies have modelled the serviceability of infrastructure systems using minimal input information on topology and logical flows but not flow-based metrics which are important for water networks to account for pressure differences in the system.

In general, previous studies have overlooked the importance of physical access to the road network in building functionality models, which is critical for post-disaster response and recovery. Additionally, limited efforts have been made in estimating interaction between household-level housing recovery and building functionality recovery modeling; when considered (e.g., Ref. [37]), the impact of household dislocation and return on infrastructure was not taken into account. To prevent or reduce service disruptions in buildings and accessibility loss to buildings, more research is needed to understand the coupled interaction between built infrastructure systems during and after disruptive events.

2.2. Infrastructure system performance

The performance of distributed infrastructure systems can be estimated using topology-based and flow-based metrics [47]. Topology-based metrics evaluate a network's mechanical connectivity using the concept of graph theory. Flow-based measures evaluate the adequacy of supplied flow volume at consumer nodes through network flow simulation. Performance measures for a particular infrastructure system are selected based on the type of services provided and their network characteristics. In some cases, topology-based functionality measures alone are not sufficient to analyze the actual behavior of infrastructure systems, which further require flow-based performance analysis to measure the serviceability at demand nodes. For instance, flow analysis is required for capturing the performance of WDS under stressed conditions after a disaster. Hence, the functionality of infrastructure systems needs to be evaluated with realistic performance measures. Moreover, the functionality of infrastructure systems is interdependent due to physical proximity, direct input-out functional linkage, shared resources, and so on [48–50]. Failure in one infrastructure system affects the performance of dependent infrastructure systems, which should be captured in estimating resilience of a community [51].

Various methods were applied in evaluating post-disaster performance recovery of infrastructure systems towards resilience modelling, including weighted operable service nodes [52], role of interdependency [20], generic network-based model [53], and multi-criteria decision-making model [31]. Ameri and van de Lindt [52] assigned weight to service nodes based on the amount of consumed service by buildings associated with service node. Guidotti et al. [20] used complex network theory to account for the independent infrastructure systems' recovery. Mohammadgholibeyki et al. [53] developed a generic network-based probabilistic recovery model of interdependent lifeline systems to avoid complex network analysis and regional seismic hazard analysis used in existing studies. Opabola and Galasso [31] presented a post-disaster recovery model for communities that considers the influence of electrical outages and building recovery pathways in developing countries, where a multi-criteria decision-making model was utilized to determine the sequencing of intervention in recovery modelling. Furthermore, major hazard events typically cause widespread damage to buildings and infrastructure components. A damaged infrastructure system is likely to suffer functionality losses to some extent and may not be able to provide adequate services to the community, which leads to essential service unavailability of buildings [54]. Simultaneously, physical damage (as well as service disruption) to one's home leads to household dislocation, and sometimes relocation, and increased service demand on essential facilities, after a disaster, which alters the demands on critical infrastructure systems throughout the restoration process and influences the performance of infrastructure systems. Social characteristics of household play a vital role in recovery of damaged buildings given differential access to recovery resources, such as insurance and different types of federal recovery aid, that can drastically speed up or slow down rebuilding timelines. Very little research focused on analyzing changes in demand on infrastructure systems, and their cascading effect on building functionality analysis [20,54,55]. Studies have quantified a household's individual make-up with sociodemographic estiamtes for residential buildings in post-disaster resilience modelling [54,56]. However, existing models do not account for demand changes due to increase service demands at essential facilities (e.g., increased demand at hospitals). Overall, community resilience analysis requires a comprehensive model that accounts for cascading failure effects in interdependent infrastructure systems, as well as post-disaster demand changes on infrastructure performance throughout the restoration process. The current study formulates a comprehensive post-earthquake functionality analysis framework to overcome existing gaps in functionality analysis of buildings and infrastructure systems, as discussed next.

3. Community resilience analysis framework

The proposed framework incorporates the performance of multiple interdependent infrastructure systems with buildings and uses an updated performance metrics to evaluate community seismic resilience. As shown in Fig. 1, the framework connects the physical systems to social systems to measure functionality of buildings by accounting for occupancy status and integrating serviceability of water and electrical power networks, and accessibility to the transportation network (TN) through roadways. Both physical and social systems are characterized using geospatial datasets. Using a scenario earthquake and Ground Motion Prediction Equation (GMPE), the framework estimates spatially distributed seismic intensities at testbed site. Damage states to buildings and infrastructure components are assigned using fragility functions, measured intensities, and random-state simulations. Physical damages are integrated into the geospatial damage layers to model interdependency between infrastructure systems and buildings. Functionality of buildings and infrastructure system is measured considering inputs from other systems. The performance of EPN is considered independent. The functionality of WDS depends on EPN serviceability (i.e., water pumping relies on electric power to operate). Therefore, the functionality of WDS is estimated considering physical damage to water pipelines and inputs from EPN. Similarly, functionality of TN is measured considering geospatial interdependency with the WDS. The functionality of buildings is estimated considering extent of physical damage and inputs from infrastructure systems. The link between physical and social systems is established by identifying the number of households occupying residential buildings. The household's sociodemographic characteristics are estimated and used to influence their predicted housing recovery experience. When building damage occurs, households often dislocate, which subsequently alters demands on the WDS. The demand changes due to household dislocation and return is accounted for through serviceability

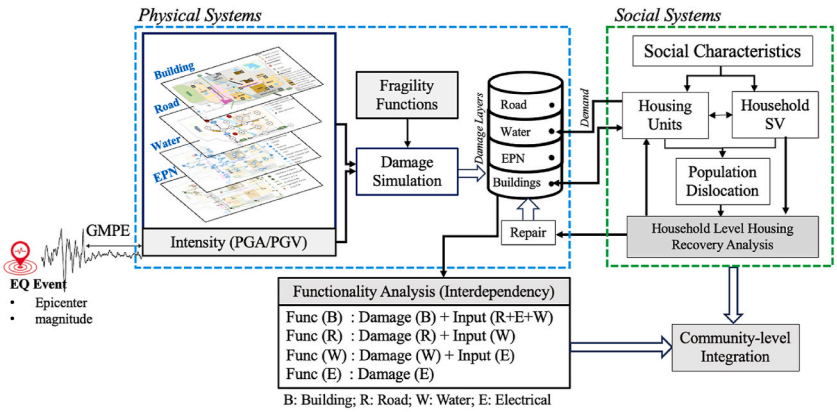

Fig. 1. Overview of proposed community-level resilience analysis framework.

analysis of WDS. Household dislocation and household-level housing recovery are modelled considering whether their home is safe to occupy and considering the household's social vulnerability (SV). During the recovery, physical system repair and household recovery are coupled to estimate community-level functional recovery.

3.1. Hazard analysis

The first step of this framework involves generating spatially distributed seismic hazard intensities to estimate probable physical damage to buildings and infrastructure systems. Using a scenario earthquake, seismic intensities at buildings and infrastructure sites are estimated using Ground Motion Prediction Equations (GMPEs) that account for uncertainties in predicted intensities. The GMPE requires scenario seismic event characteristics, including magnitude, epicenter location, distance between epicenter and site, fault characteristics, and site condition. Intensity measures (e.g., peak ground acceleration) can be selected based on the vulnerability associated with the structural systems of interest.

3.2. Vulnerability analysis

In the second step, the seismic vulnerability of buildings and infrastructure components is evaluated by estimating the expected performance levels (measured here by damage states (DS)) against a given seismic intensity. Fragility functions are commonly used to determine the expected structural performance levels where probabilities of exceeding various DSs of a structure are conditioned on estimated seismic intensity. This study uses four DSs (i.e., slight, moderate, extensive, and complete) for aboveground structures and two DSs (i.e., leak and break) for buried pipelines from literature, as described in Table 1.

3.2.1. Fragility functions

Fragility functions are typically defined using lognormal cumulative distributed functions. The fragility function for a DS can be defined as [57]:

$$F_r(DS|im) = \varphi\left[\ln\left(\frac{im}{\lambda}\right) \Big/ \zeta\right] \tag{1}$$

Table 1
Damage State definitions.

Structural System	Description	Reference
Buildings/Bridges/Water Tank/ Substations/Poles	**None:** no visible non-structural or structural damage is visible. **Slight (DS1):** minor cracks, spackling, fallen contents, etc. No structural repair is required. **Moderate (DS2):** reparable structural damage to structural components without substantial demolition. **Extensive (DS3):** large diagonal cracks in structural elements; permanent lateral movement of structural components; cracks in foundations; structurally inoperable. **Complete (DS4):** structure may have large permanent displacement or failure of the lateral load resisting system; large foundation cracks; collapsing and losing the total of its contents.	FEMA [57]; Nielson and DesRoches [58]
Pipelines	None: no structural damage to pipeline. Leak: enables unwanted water escaping from the pipeline by means other than through a controlled action; still able to provide service with water. Break: suffers breaks in some way and is unable to provide water flow/service.	ALA [59]

where φ is the standard normal cumulative distribution function, λ and ζ are median capacity and logarithm standard deviation and *im* is intensity measure.

Expected probabilities of DS for aboveground structures, including buildings, bridges, elevated water tanks, electrical poles, etc., are estimated using lognormal fragility functions. On the other hand, damage states for buried pipelines are estimated using empirically observed damage data fitted to Poisson functions [59]. Fig. 2 shows an example of typical lognormal and Poisson fragility curves for structures.

3.2.2. Damage simulation

DS to buildings and infrastructure components is assigned through a stochastic simulation. Probabilities of exceeding various DSs are estimated using appropriate fragility functions given estimated seismic intensity. Fig. 2 shows generalized fragility curves for buildings and infrastructure components. Four types of seismic damage states (DS) are typically determined for buildings and infrastructure components, except for pipelines. Two types of DS, namely leak and break, may occur in buried pipelines. A DS is assigned to each building or infrastructure component by comparing the fragility functions, seismic intensities, and a randomly generated number on a uniform distribution U[0,1] in stochastic realization. The intersection of x-axis (i.e., earthquake intensity) and y-axis (i.e., random number) values is mapped on fragility curves to determine the damage state for a particular building or component for a single stochastic realization [60,61], as illustrated in Fig. 2.

3.3. Functionality analysis

Functionality is measured by the ability of buildings or infrastructure systems to serve their intended purpose [38,42]. Following a disruptive event, the framework assesses the functionality of buildings, EPN, WDS, and TN, incorporating cascading effects and interdependency between them.

3.3.1. Buildings

It is assumed that a building experiencing DS either extensive or complete will be unsafe to occupy [18]. The functionality states of buildings are defined based on the physical operability (O_B) (i.e., if the building sustained none, minor or moderate damage), availability of water (S_W) and electrical power (S_E) services, and physical accessibility to the road network (A_R). Three functionality states of building (FSB) are adopted herein, as follows.

$$\mathrm{FSB_i} = \begin{cases} \text{Fully Functional}, & \text{case when } \mathrm{O_B} \cap \mathrm{S_E} \cap \mathrm{S_W} \cap \mathrm{A_R} \\ \text{Partially Functional}, & \text{case when } \mathrm{O_B} \cap \mathrm{S_E} \cap \mathrm{S_W} \cap \overline{\mathrm{A_R}} \\ \text{Non} - \text{Functional}, & \text{case when } \overline{\mathrm{O_B}} \cap (\overline{\mathrm{S_E}} \cup \overline{\mathrm{S_W}}) \end{cases} \tag{2}$$

where building-*i* is fully functional if the building is physically safe to occupy and having minimal level of required water and electricity and has physical access to nearest road segment; building-*i* is partially functional if the building is operable and has water and electricity but lost physical access to nearest road segment; and building-*i* is non-functional if building at least sustain higher $\geq$ DS3 or experience either water or electricity outage.

Fig. 3 illustrates the dependency of buildings on EPN, WDS, and TN, as well as the interdependency between them. FSB is measured using equation (2). Water and electrical availability to a building are mapped based on the functionality of the corresponding service area, as discussed later in this paper. Physical accessibility to the nearest road segment is estimated using the shortest path method. Household Social Vulnerability (SV) plays an important role in their decision to dislocate from damaged buildings and their recovery, which is captured through an existing Household-level Housing Recovery (HHHR) model [62]. The results of physical damage repair and housing recovery are coupled to determine a realistic return to their homes. A dislocated household recovered from the HHHR model will return to their original home as long as their building becomes operable or safe to occupy after repair. Otherwise, a dislocated household needs to wait in temporary housing until their damaged home is repaired. On the other hand, if a dislocated household is permanently unable to recover, the repair analysis assumes that the building will never recover and be abandoned.

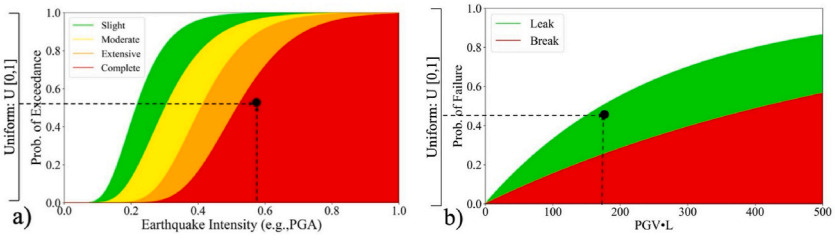

Fig. 2. Stochastic damage simulation for: a) buildings/bridges/water tanks/electrical substations, and b) pipelines.

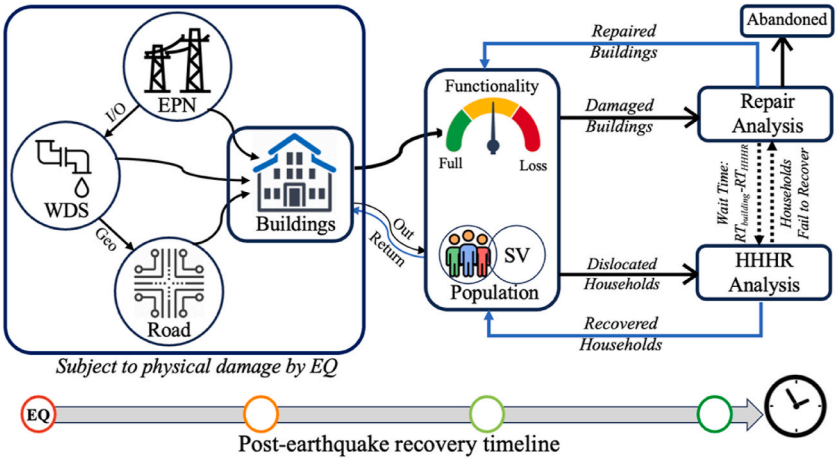

Fig. 3. Interdependency and Functionality of Building at time - *i*.

Damage repair and HHHR analysis are performed to simulate post-earthquake recovery until the community returns to its near pre-disaster state (indicated by the timeline in Fig. 3).

Communities consist of numerous buildings of various occupancies and structural types, which collectively support the functionality of a community. To aggregate the functionality of buildings in a zone, the portfolio-level building recovery is defined as a ratio of functional buildings to total buildings evaluated at any given time. The building portfolio functionality is expressed by the following equation from Lin and Wang [63]:

$$FP_j(t) = \frac{\sum_{i=1}^{N} FSB_i^j(t)}{N} \tag{3}$$

where $FP_j(t)$ is the portfolio functionality of the *j*-th building zone at time *t*; N is the total number of buildings in the zone; FSB_i is the binary functionality state of i-th building, as defined in equation (2).

3.3.2. *Infrastructure systems*

The system-level functionality of infrastructure systems is evaluated by estimating topology-based performance metrics and hydraulic availability. In EPN, substations are the weakest components when exposed to seismic loading; research has shown that the seismic vulnerability of transmission lines can be considered negligible [64]. Therefore, the damage to EPN is determined for the electrical substations only. The functionality of the EPN is estimated by the percentage of service nodes (i.e., electrical poles) that remain connected to a source (i.e., distribution substation) after an earthquake. For the WDS and TN, the vulnerability is mainly determined for links (i.e., pipe, road segment). Therefore, the system-level functionality of WDS and TN is measured by the network efficiency metric which evaluates network performance using the shortest-path algorithm. Infrastructure networks are modelled using graph theory where an edge of a network graph represents pipe/road segment/wire, and a vertex of a network graph represents service nodes (i.e., nodes, poles, junctions, tanks).

3.3.2.1. Network connectivity. The network connectivity determines percentage of demand/service nodes are physically connected to source. Connectivity depends on the topological layout of the network and the possible optimal flow patterns. Network connectivity estimation does not rely on the physical characteristics of the network but can capture demand and supply of flow constraints to some extent [65]. This measure is widely used to evaluate the functionality of a network after perturbation [21]. The following equation estimates the connectivity (n_c) of a network.

$$n_c = \frac{1}{n_{demand}} \sum_{i}^{n_{demand}} \frac{P_i}{P_{i,0}} \tag{4}$$

where P_i is the number of source nodes connected to a demand node, $P_{i,0}$ is the number of source nodes connected to *i*-th node before failure, and n_{demand} is the number of demand nodes.

3.3.2.2. Network efficiency. The network efficiency estimates the coordination of nodes within the network as a function of the average shortest path distance. The shortest distance among nodes is likely to increase in case of failure of link(s) in a network, reducing the overall coordination among nodes and the network's performance [66]. The shortest path-based network efficiency is a powerful tool to analyze the topological effectiveness of a network after perturbation and during recovery. The network efficiency is measured by the following expression [67]:

$$\eta(G) = \frac{1}{n(n-1)} \sum_{i=1}^{n} \sum_{\substack{j=1 \\ i \neq 1}}^{n} \frac{1}{d_{ij}} \tag{5}$$

where $\eta(G)$ is the network efficiency at time t; d_{ij} is the shortest path between node i and node j; n is the number of nodes in the network. If the node i is disconnected from the node j, then d_{ij} becomes infinity (∞).

3.3.2.3. Hydraulic availability. WDS's ability to provide a satisfactory amount of water service without interruption not only depends on connectivity but also depends on the pressure at demand nodes. The hydraulic availability at a demand node is estimated by the actual water supplied. The available water volume at a demand node is correlated with pressure at the node. A pressure-driven hydraulic simulation is performed to capture actual water flows at demand node under partially failed conditions [68]. The following equation developed by Wagner et al. [69] is used to estimate actual supplied water volume at demand node:

$$Q_j^a = \begin{cases} 0 \,; p \leq P_m \\ Q_j^{req} \sqrt{\frac{p - P_m}{P_s - P_m}}; \; P_m \leq p \leq P_s \\ Q_j^{req}; p \geq P_s \end{cases} \tag{6}$$

where Q_j^a is the actual supplied water at node j; Q_j^{req} is the required water demand at node j; P_s is the required pressure at node j to supply required volume of water; P_m is the minimum required pressure to supply water, below this level, the node will not receive any water; p is the pressure at demand node j. If a node's required pressure is satisfied, the node will be able to provide adequate supply to all dependent households. Q_j^a values less than 1 represent partial water supply meaning the household will receive water.

3.3.2.4. Dislocation and demand changes. Physical damage to buildings may result in household dislocation and an increase in service demands on critical facilities (e.g., hospitals), which must be accounted for in altered demands assignment and serviceability analysis of the WDS. Buildings with severe or extensive damage are marked as inoperable; hence, residents in these buildings are dislocated immediately after the disaster. Buildings experiencing moderate damage have safety concerns, and residents in these buildings may dislocate. The building damage level and the household's SV are used to estimate the households' probability to dislocate [54]. Households with low SV may choose to leave their home until repaired, whereas households with high SV typically have fewer relocation choices due to fewer resources. The SV of each household is assigned on a scale of [0,1] based on their socioeconomic attributes (e.g., race, ethnicity, income, tenure status, etc.), where the maximum value represents the highest SV [62,70]. Expanded from the Sutley and Hamideh [62] original work, here, households dislocate if they have an SV lower than a specified threshold and a damaged home that reaches or exceeds moderate damage. Household dislocation and return are accounted for through demand changes to the WDS hydraulic model throughout the recovery process. Increased post-earthquake demands on critical facilities can be accounted for by an adjustment factor based on service type, capacity, and more.

3.3.2.5. Interdependency. The functionality analysis of buildings needs to measure the availability of the WDS and EPN and accessibility to the nearest road segment, whereas infrastructure systems are interdependent on each other. As shown in Fig. 3, WDS requires electrical power for pumping stations to ensure pumping operation for an adequate water supply. Input-output (I-O) interdependency is considered between EPN and WDS. Roads and water pipelines are often physically collocated, and the failure of a water pipe is likely to interrupt nearby road operations due to the close physical proximity among them. Geospatial analysis is performed to account for WDS and TN proximity. A 10-m buffer offset is set in the Geographic Information System (GIS) from the centerline of the water pipelines to identify the intersecting road segments within buffer zones [50]. It is assumed that collocated road segments will be closed for damaged water pipe repairs. Inoperable links and nodes are removed from the network while estimating the performance of these networks. Infrastructure I-O interdependency is modelled as follows:

$$q = Z(G)q + \overline{\overline{f}} \tag{7}$$

where q is the non-functionality vector resulting due to perturbation in individual network's $Z(G)$ non-functional components $\overline{\overline{f}}$ (i.e., perturbation vector). The non-functionality vector q can be estimated as

$$q = (1 - Z(G))^{T-1} \overline{\overline{f}} \tag{8}$$

3.3.2.6. Service area. Service area for each infrastructure system can be determined using various approaches, including Cellular Automata Algorithm, Graph Approximation and Voronoi Polygons, etc. [71,72]. In this study, service areas for infrastructure systems are estimated using Voronoi polygons [73]. Service area is approximated based on primary service nodes (e.g., water nodes, substations) within the study area. EPN and WDS service to buildings within a specific service area comes through associated primary node. Hence, if a primary service node is out of service, the buildings within the same service area will not receive service from that

network. For road network, the shortest path distance is used to identify the primary and nearest road segment accessibility. Using this approach, the serviceability of WDS/EPN nodes (i.e., S_W, S_E) and road segments (i.e., A_R) are mapped to associated building's operability to determine the functionality of building.

3.4. Restoration analysis

3.4.1. Physical Damage repair

Damaged structures need to be repaired following a disaster. The time required to repair a damaged building or infrastructure component depends on the extent of physical damage and available resources (e.g., repair crew availability, accessibility, travel to site, weather, equipment availability, financial resources). Expected repair time for damaged structural components can be adapted from literature. This study utilizes mean repair time for damaged buildings and infrastructure components documented in FEMA [57] and Porter [74] to simulates a feasible long-term recovery approach assuming recovery resources are eventually allocated to each system, and only one repair could be performed at a time (Mazumder et al., 2022). Repair time is simulated through a Monte Carlo simulation where uncertainty associated to repair process is accounted for assuming repair time follows normal distribution based on the expected repair time and standard deviation [21].

3.4.2. Household level housing recovery

A household's housing recovery process depends on myriad factors, including the household's social vulnerability, financial recovery resources, and the extent of damage to their home, among other factors [62]. Here, a household can be defined as a group of individuals who live together in a single dwelling, sharing spaces and functioning as a single unit. This may include a family, roommates, or any other group of people who reside together. A household can consist of either one person or multiple people living together. Here a household-level housing recovery trajectory is predicted using the model developed by Sutley and Hamideh [62]. The household recovery sequence is modelled using a modified Markov chain capturing movement through five discreet states: emergency shelter (S1), temporary shelter (S2), temporary housing (S3), permanent housing (S4), and failure to recover (S5). Transition probabilities are a function of the household's Social Vulnerability (SV); rules are used to determine when to send a household to S5 for languishing in unstable housing. This model is applied here to estimate the housing recovery sequence of single-family household only. Required sociodemographic characteristics of households can be attained from census and other public data sources.

3.5. Algorithms

The proposed framework is executed through developing a Python script coupled with geospatial analysis conducted within a GIS environment. The stepwise procedures of the framework at each recovery time-step are depicted in Fig. 4.

Algorithm for Community-Level Functionality Analysis

1. **Inputs**: Buildings, Bridges, Tanks, Pipes, Substations (Geodatabase – coordinates, structural types); n_b: number of buildings, n_s: number of substations, n_t: number of tanks, n_p: number of pipes, n_{br}: number of bridges, N: all structures
2. **Estimate Seismic Intensities at Site:** (Ground Motion Prediction Equation - Magnitude, Epicentral Depth and Location of Earthquake, Distance to Site)
3. **Define Fragility Curves for Structures and Simulate Damage**:
4. Calculate DS probabilities P_{fi} for all structure i in [1:N] given intensity
5. Generate random numbers on uniform U[0,1] for all structure i in [1:N] and compare with DS probabilities and assign DS_i
6. **Estimate Household Dislocation**: check for all buildings - j in [1: n_b]:
7. if ($DS_j \geq 3$ is true and building structural archetype = 'RES') then household dislocate
8. **Find Damaged in EPN:** check for all substations - k in [1: n_s]:
9. if ($DS_k \geq 3$) is true then remove substations from EPN, and remove dependent pumps from WDS
10. assign electrical outage to dependent buildings found using Voronoi polygons
11. **Estimate Damage in WDS:** check for (Break or Leak) in all pipes - x in [1: n_p]:
12. if (Break or Leak) is true then remove the pipe from WDS, and remove road segment(s) within 10 m buffer from center of the pipe
13. check for all tanks - y in [1: n_t]:
14. if ($DS \geq 3$) is true then remove the tank from WDS
15. **Estimate Damage in TN**: check for all bridges - b in [1: n_{br}]:
16. if ($DS \geq 3$) is true then remove road segment contains the bridge
17. **Adjust demands of service nodes:** based on household dislocation outputs (from steps 6-7) and to essential facility
18. perform WDS hydraulic simulation - estimate serviceability to all buildings (using Voronoi polygons & hydraulic simulation results)
19. **GIS – network analysis :** (i) find buildings that lost accessibility to nearest road segment (due to road closure found in steps 12 & 16)
20. (ii) find buildings within electricity outage area (Voronoi polygons with no electrical serviceability - from step 10)
21. **Estimate functionality :** (i) individual building (eq. 2)
22. (ii) community-level functionality (eq. 3)
23. (iii) system-level network performance (eq. 4-5)
24. **Repair Simulations** : (i) estimate repair time of damaged structures based on mean repair time (from Table 6 & MCS).
25. (ii) repaired structure added back to original system
26. **Perform Household-level Housing Recovery analysis:** for dislocated households estimated in steps (6-7)
27. (i) If household recovery time < building repair time: household waits for repair to be completed
28. (ii) If a household fails to recover: building remain at the same FS and become abandoned
29. **Re-estimate and update functionality**

Fig. 4. Steps of the proposed framework at each recovery time-step.

4. Illustrative analysis

The proposed community resilience analysis framework is demonstrated using the Centerville virtual testbed [75]. Centerville represents a typical mid-size community in the midwestern USA over an area of approximately 100 km^2. Four types of physical infrastructure systems (i.e., buildings, electrical, water, and road) are modelled as Centerville's built environment (see Fig. 5). The building portfolio contains 15,130 buildings and 20,484 households in 7 residential zones, 2 commercial zones, 2 industrial zones, 19 essential facilities (i.e., regional hospital, fire stations, schools, etc.). An estimated 52,029 people live in the seven residential zones. These residential zones are categorized according to the income level of the residents as well as the building density. The two commercial zones are located along major roadways. The light industrial zone is located at the north of the community, while the heavy industrial zone is located at the southeast of the community. Table 2 reports the number of buildings, households, people and mean SV of households by zone.

4.1. Service area and interdependency

Fig. 6(a)–6(c) show the service area of the EPN and WDS, as well as the nearest road segments from buildings. By employing Voronoi polygons, we ascertain the service areas for EPN and WDS, where infrastructure services emanate from specific primary service/demand nodes. If a service/demand node becomes non-functional, the buildings within the corresponding service area will no longer receive that service. The physical I-O linkage is assessed to determine the physical interdependency between EPN and WDS, and geographic interdependency is measured for WDS and TN. For EPN and WDS, three pumping stations PS1, PS2, and PS3 operation dependent on electrical service from electrical poles P28, P19 and P15, respectively, where substation P8 feeds pole P15 and substation P27 feeds pole P28 (see Figs. 4 and 6(a)–(b)). Therefore, service outage in P8, P15, P19, P27 and P28 will result in cascading service failures in the WDS. A 10m buffer alongside the center of pipelines is drawn to determine road segments collocated to water pipes. As shown Fig. 6(d), red segments within the buffer are termed as collocated road segments, meaning failure of any pipelines within this buffer will result in closure of collocated road segments for pipeline repair works.

4.2. Hazard and physical Damage analysis

A hypothetical M_w 7.8 earthquake scenario with an epicenter located approximately 20 km southwest of Centerville is simulated. Peak Ground Acceleration (PGA) is estimated for measuring damage to buildings and most infrastructure components. Since seismic wave propagation is the main cause of buried pipeline damage, Peak Ground Velocity (PGV) is measured to evaluate the seismic performance of buried pipelines [4]. Seismic intensities at sites are generated using GMPEs developed by Kawashima et al. [76] and Yu and Jin [77], as expressed by following equations

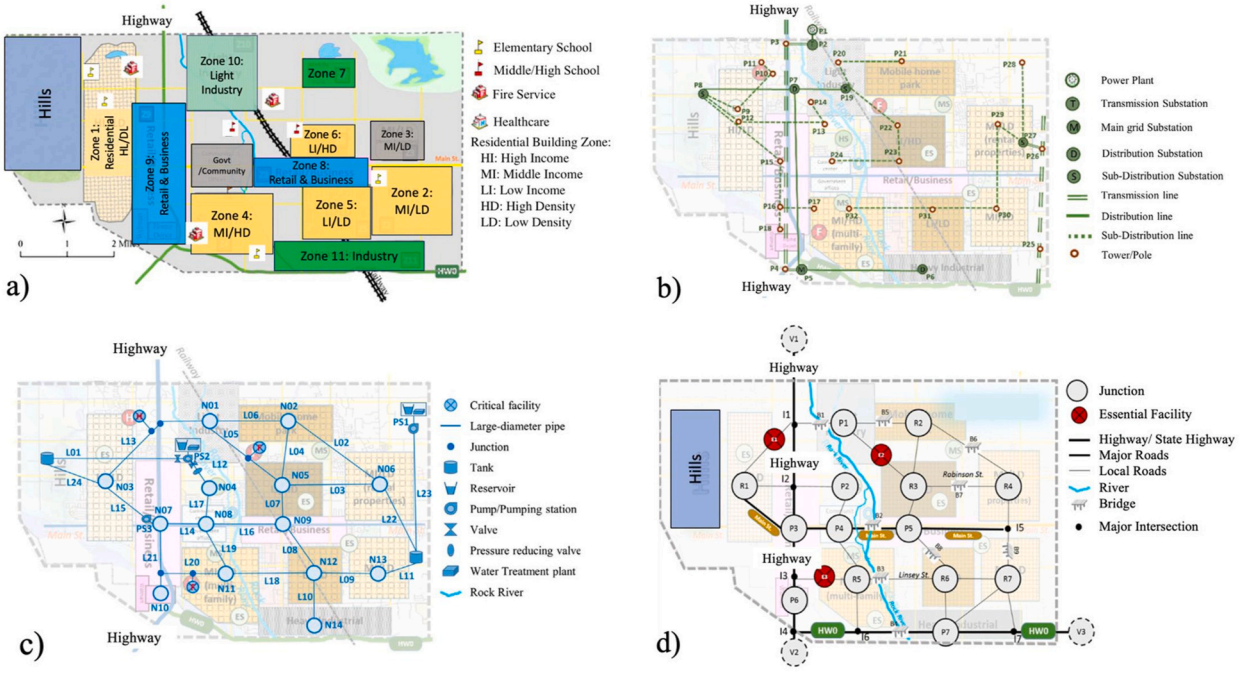

Fig. 5. Centerville Testbed: a) buildings, b) EPN, c) WDS, and d) TN (Adapted from Ref. [75]).

Table 2
Number of buildings, households and population.

Zone ID	Buildings	Households	Population	Mean SV
Z1	4246	4246	10,785	0.17
Z2	2267	3067	7790	0.19
Z3	800	800	2032	0.34
Z4	3592	4767	12,108	0.42
Z5	1856	1856	4714	0.62
Z6	777	4396	11,166	0.37
Z7	1352	1352	3434	0.35
Z8	57	Retail/Business		–
Z9	94	Retail/Business		–
Z10	25	Light Industry		–
Z11	45	Heavy Industry		–
–	19	Essential Facilities (Schools/Hospital/Fire Station/Govt.)		–
Total	**15,130**	**20,484**	**52,029**	

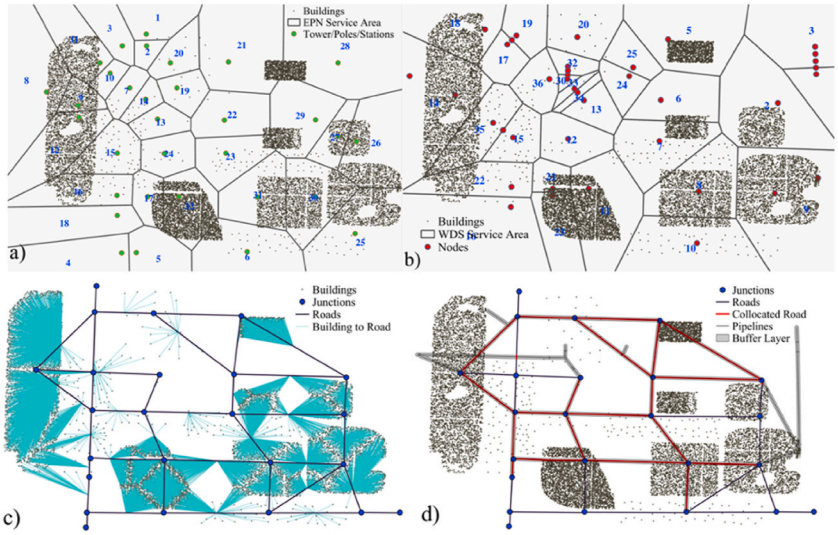

Fig. 6. Centerville physical systems: a) EPN service area, b) WDS service area, c) buildings to nearest road segments, and d) TN and WDS interdependency.

$$PGA = 403.8 \times 10^{0.265M}(R+30)^{-1.218} \quad (9)$$

$$PGV = 10^{-0.848+0.775M+1.834\ \log(R+17)} \quad (10)$$

where PGA and PGV are expressed in cm/s^2 and cm/s, respectively; M is the magnitude; R is the distance from epicenter expressed in km. Then, the damage for physical systems is simulated using estimated seismic intensity, fragility functions, and randomly generated numbers, as described in section 3.2.2.

4.2.1. Electrical power network

Centerville EPN consists of 1 power plant, 1 transmission substation, 1 main grid substation, 5 distribution substations, and 24 towers or poles connected by transmission, distribution, and sub-distribution lines. Fig. 7(a) shows various components of EPN and the associated service area. Seismic vulnerability is considered negligible for electrical lines, and damage states are [64]. Hence, seismic damage was estimated for substations only. Fragility functions for electrical substations are adapted from FEMA [57], as shown in Table A1. The cascading effect of any substation failure was determined by analyzing the connectivity of substations and electrical poles/towers. For instance, the failure of distribution substation P8 leads to the functionality loss of dependent poles P9-P18 (see Fig. 4 (b)). Estimated PGA and DS for EPN are shown in Fig. 7(b) and (c), respectively. Southwest part of the Centerville experienced higher seismic intensities due to scenario earthquake. Substation P8 and distribution station P6 suffered extensive damage, resulting in electrical outage in a large part of Centerville, as shown in Fig. 7(d). These two distribution substations (i.e., P8 & P6) are located in zones with lower level of social vulnerability compared to transmission substation (P7) and main grid substation (P5) (see Appendix A1). However, higher level of damages to these substations, P8 and P6, are due to higher seismic intensities, and

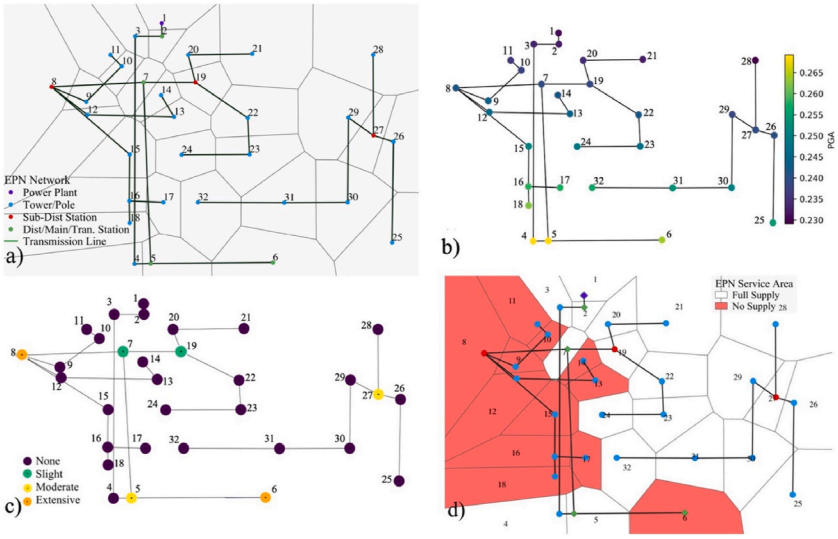

Fig. 7. Electrical Power Network: a) network and service area, b) PGA, c) damage states, and d) power outage area after earthquake.

uncertainties associated with scenario event simulation. Buildings and pumping stations depended on substations P8 and P6 suffer electrical outages. Other stations that experienced slight or moderate damages remain functional after the earthquake.

4.2.2. Water Distribution System

Centerville WDS consists of 14 demand nodes, 2 tanks, and 5 junctions connected by 24 large-diameter pipelines. Fig. 8(a) shows components of WDS and their service area. Seismic damage to WDS was simulated for the buried water pipelines and elevated water tanks. The fragility functions for buried water pipelines are defined based on American Lifeline Alliance (ALA) 2001 guideline. The failure probability of pipe leakages and breaks are estimated as follows [61].

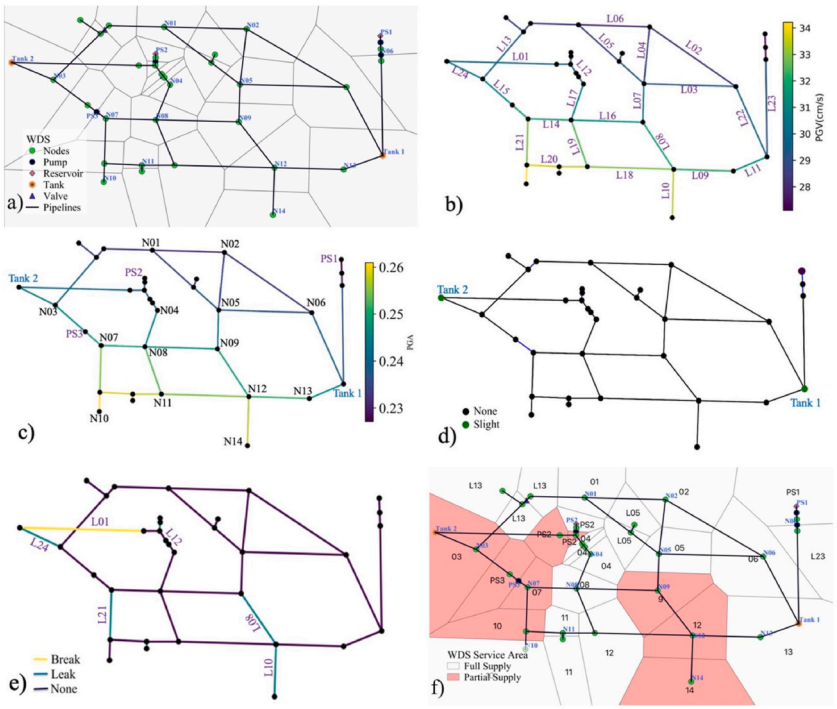

Fig. 8. Water Distribution System; a) network and service area, b) PGA, c) PGV, d) damage states of tanks, e) damage states of pipes, and f) impacted service area.

$$P_{leak} = 1 - e^{-RR \times L} \tag{8}$$

$$P_{break} = 0.25 \times P_{leak} \tag{9}$$

where repair rate, RR is estimated by $k_1 \times 0.00187 \times$ PGV for every 1000 ft; PGV is in inch per second; k_1 is the correction factor for pipe material, size, joint, and soil type [59].

Fig. 8(b) and 8(c) show estimated PGA and PGV values for water tanks and pipelines, respectively. Fragility functions provided in Equations (8) and (9) and Table A1 were used to determine damage to pipelines and tanks, respectively. Fig. 8(d) and (e) show DS for water tanks and pipelines, respectively. None of the tanks experienced severe or extensive damage; hence, both tanks remain functional after the earthquake. One pipe experienced a break (pipeline with yellow color), and 6 pipes experienced leaks (pipelines with green color) due to the earthquake, as shown in Fig. 8(e). Fig. 8(f) shows the service area that suffered some extent of water serviceability loss due to damage in the WDS.

4.2.3. Transportation network

Centerville TN consists of interstate/state highways, major roads, and 9 bridges, as shown in Fig. 9(a). Major roadways connected to various zones can be seen from Fig. 4(d). The most vulnerable component of TN against earthquakes is the bridge. Seismic damage to TN was evaluated for bridges only. It is assumed that if a bridge is damaged, then the road segment containing the bridge will be closed due to bridge repair work. DS to bridges are assigned using fragility functions developed by Nielson and DesRoches [58], and stochastic analysis. Fig. 9(b) shows the estimated PGA for TN. Two bridges (B3 and B7 in Fig. 4(c)) experienced extensive and complete damage, and therefore became inoperable after the earthquake. Four bridges experienced either slight or moderate damage and remain functional after the earthquake. Fig. 9(c) shows DS of bridges. Fig. 9(d) shows links from closed road segments to the nearest buildings using the shortest path method. These buildings will experience a physical accessibility burden; hence, their travel time after the disaster will significantly increase through an alternative route, if available.

4.2.4. Buildings

Centerville's building inventory consists of 16 structural archetypes for 11 building occupancy types, including residential, commercial, industrial, and critical facilities such as hospitals, fire stations, schools, and government offices. A total of 15,130 buildings, including 19 critical facilities, are distributed over 7 residential zones, 2 commercial zones, and 2 industrial zones (1 light industry and 1 heavy industry), as shown in Fig. 10(a). Fragility parameters for the archetypes are adapted from FEMA [57] and provided in Table A2.

Fig. 10(b) and (c) show estimated PGA using GMPE provide in Eq. (9) and DS of buildings, respectively. It should be noted that the seismic intensity was estimated based on a single instance of hazard and a single instance of damage. Table 3 summarizes building DSs. Approximately 20.6 % of total buildings suffered either extensive or complete damage, leaving the buildings unsafe to occupy after the earthquake.

4.3. Repair analysis

The mean repair time for buildings, EPN, and water tanks is adapted from FEMA [57], and the mean repair time for pipelines is adapted from Porter [74]. It is assumed that each utility has enough resources to repair one damaged component at a time during the recovery process (as opposed to simultaneously). Uncertainty in the repair process is considered through a Monte Carlo Simulation

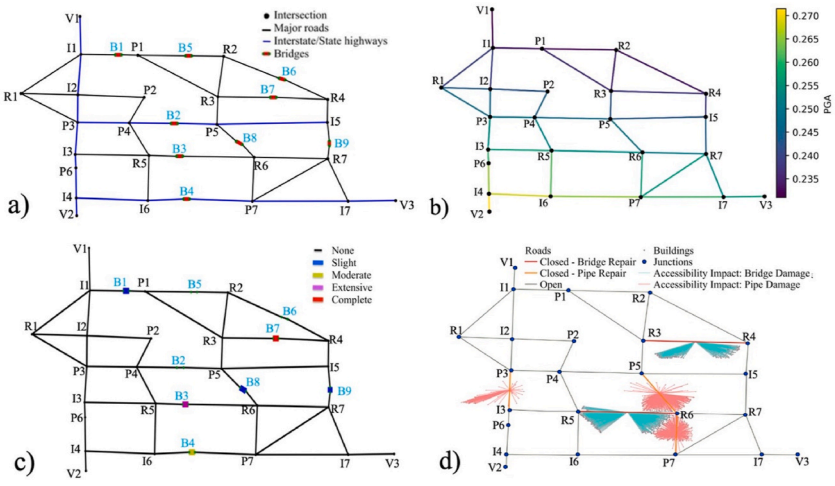

Fig. 9. Transportation Network: a) components, b) PGA, c) damage states, and d) buildings experiencing accessibility loss to nearest road segment after earthquake.

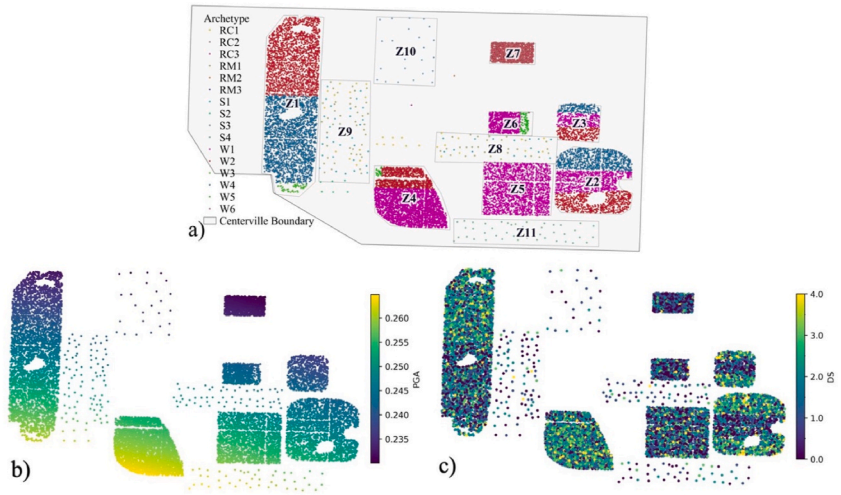

Fig. 10. Buildings: (a) distribution of building structural archetypes; (b) PGA; and (c) damage states (0: None; 1: Slight; 2: Moderate; 3:Extensive; 4:Complete).

Table 3
Building damage states.

Damage State	No. of Buildings (%)	No. of Households (%)
None	3532 (23.3 %)	5356 (26.2 %)
Slight	3799 (25.1 %)	5990 (29.2 %)
Moderate	4713 (31.2 %)	5557 (27.1 %)
Extensive	2147 (14.2 %)	2465 (12.0 %)
Complete	939 (6.2 %)	1106 (5.4 %)
Total	**15,130**	**100.0 %**

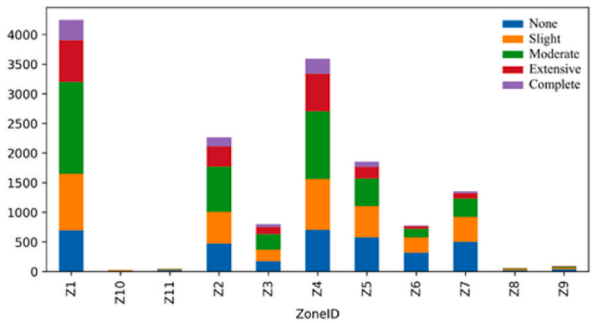

Table 4
Mean repair time (days) adapted from FEMA [57] and Porter [74].

Structure	Types	Minor	Moderate	Extensive	Complete
Building	RES1	5.0 (1.5)	120.0 (36.0)	360.0 (108.0)	720.0 (216.0)
	RES2	5.0 (1.5)	20.0 (7.0)	120.0 (36.0)	240.0 (72.0)
	RES3	10.0 (3.0)	120 (36.0)	480.0 (144.0)	960.0 (288.0)
	COM1/COM3	10.0 (3.0)	90.0 (27.0)	270.0 (81.0)	360.0 (108.0)
	COM4	20.0 (7.0)	90.0 (27.0)	360.0 (108.0)	480.0 (144.0)
	COM6	20.0 (7.0)	135.0 (40.5)	540.0 (162.0)	720.0 (216.0)
	IND1/IND2	10.0 (3.0)	90.0 (27.0)	240.0 (72.0)	360.0 (108.0)
	GOV2	10.0 (3.0)	60.0 (18.0)	270.0 (81.0)	360.0 (108.0)
	EDU1	10.0 (3.0)	90.0 (27.0)	360.0 (108.0)	480.0 (144.0)
EPN	Transmission Substation	1 (0.5)	3.0 (1.5)	7.0 (3.5)	30.0 (15.0)
	Main/Sub-grid Substation	1 (0.5)	3.0 (1.5)	7.0 (3.5)	30.0 (15.0)
TN	MSC Concrete Bridge	0.6 (0.6)	2.5 (2.7)	75.0 (42.0)	230.0 (110.0)
	MSSS Concrete Bridge	0.6 (0.6)	2.5 (2.7)	75.0 (42.0)	230.0 (110.0)
WDS	Tank	1.2 (0.4)	3 (2.7)	93 (85)	155 (120)
			Leak		Break
	Pipe (<20 in. Diameter)	–	0.34 (0.10)	–	0.50 (0.15)
	Pipe (>20 in. Diameter)	–	0.50 (0.15)	–	1.33 (0.40)

Note: all restoration functions are normal distribution where mean (standard deviation) are provided. RES: Residential; COM: Commercial; IND: Industrial; GOV: Government; EDU: Educational.

where a coefficient of variation of 0.3 is assumed. The mean repair time and standard deviation by structure type are provided in Table 4. Repair analysis outcomes were used to update changes in demand on the WDS throughout the repair process. The Monte Carlo process generates 10,000 samples for each damaged building or structural component, where the mean value of the generated numbers is considered the repair time for damaged building or component. It should be noted that the expected building repair time also includes potential delays in decision-making, financing, and the inspection process [57].

4.4. Functionality restoration analysis

4.4.1. System-level functionality restoration of infrastructure systems

The functionality of infrastructure systems was determined using connectivity and network efficiency, as described in section 3.3.2. The system-level performance of the EPN is measured by network connectivity, and the performance of the WDS and TN is measured by network efficiency. The Networkx python tool was used to estimate network efficiency and analyze connectivity [78]. Fig. 11 shows post-earthquake system-level functionality restoration of infrastructure systems. The scenario earthquake resulted in extensive damage to substations P8 and P6. The failure of P8 leads to an outage of eight dependent poles and subsequent power outage in zones Z1, Z4, Z9, one high school, and hospital buildings. The failure of station P6 leads to an electrical power outage in Z11. The connectivity of EPN drops about 40 % due to the failure of substations P8 and P6. Two repair sequences, S1[repairing P8 first followed by P6] and S2 [repair P6 first followed by P8 repair], were considered to estimate functionality recovery of EPN, as shown in Fig. 11(a). Since repairing sub-distribution station P8 restores electrical power service to a large part of Centerville, the sequence S1[P8, P6] provides higher functionality recover during the repair process.

The water pipes repair sequence is developed based on typical asset repair practice where a pipeline experiencing a break is repaired first followed by repairing leaky pipes. Leaky pipelines were prioritized for repair based on their serviceability to essential facilities. Table 5 shows the repair sequence and corresponding repair time of WDS. Water tanks experiencing minor damages are repaired after repairing all damaged pipelines. Fig. 11(b) shows post-earthquake network efficiency of WDS. Immediately after the earthquake, network efficiency drops about 24 %, and more than 6 days were required to recover completely. Also, dependency on water pumping on EPN was considered. Due to the outage at sub-station P8 and pole P15, pump station PS3 experienced an electrical outage for 7 days after the earthquake, lasting until station P8 was repaired. Pump stations PS1 and PS2 did not experience any power outage.

In TN, bridges B3 and B7 experienced extensive and complete damage, respectively, leading to the closure of road segments R3-R4 and R5-R6. Three possible repair sequences (S1[#3, #7], S2[#7, #3], and concurrent repair) were considered for estimating functionality recovery of TN, as shown in Fig. 11(c). Repairing the extensively damaged bridge B3 takes a relatively shorter period than the time to repair the completely damaged bridge B7. Repair following sequence S1[#3, #7] provides higher functionality than the repair following sequence S2[#7, #3]. Repairing two bridges simultaneously requires 230 days, whereas repairing one bridge at a time requires 305 days to complete the repair process. Although the other four bridges experience either slight or moderate damage, they

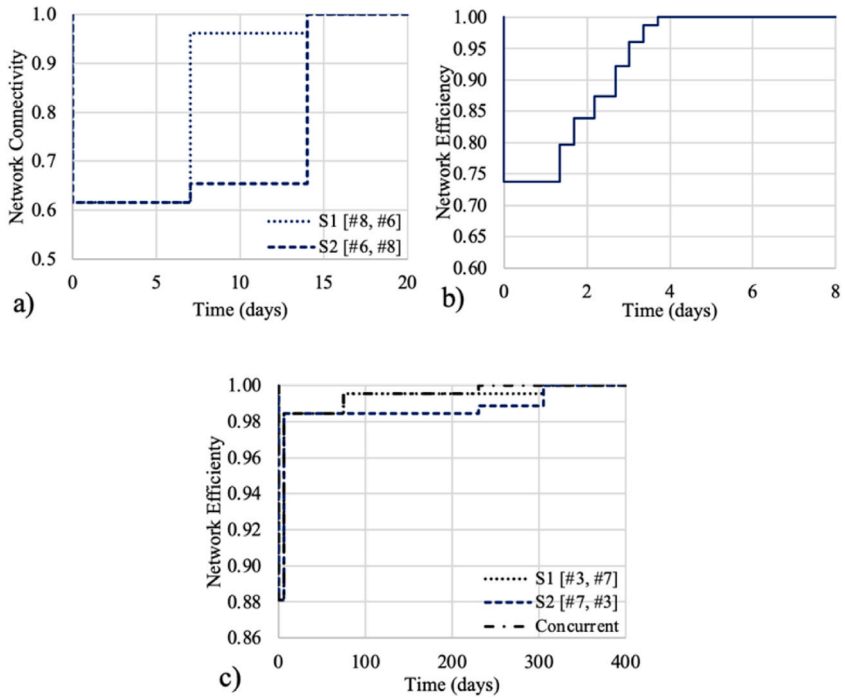

Fig. 11. Post-earthquake functionality of (a) EPN, (b) WDS and (c) TN.

Table 5
Repair of WDS.

Sl.	Pipe Type	Pipe #	Feeding to	Damage	Days	Cumulative Days
1	Large	L01	Break, hospital, water treatment plant	Break	1.34	1.34
2	Small	L20	Fire Station	Leak	0.34	1.68
3	Large	L12	Tank, pump station	Leak	0.50	2.18
4	Large	L08	Residential	Leak	0.50	2.68
5	Small	L24	Residential, reservoir	Leak	0.34	3.02
6	Small	L10	Industrial Zone	Leak	0.34	3.36
7	Small	L21	Residential	Leak	0.34	3.70
8	Tank	#1	Source	Slight	1.20	4.90
9	Tank	#2	Source	Slight	1.20	6.10

remain functional during and after the earthquake. The failure of two bridges decreases network efficiency and increases travel delays. Since there is redundancy, the network efficiency drops slightly (about 1.5 %) due to the failure of two bridges. However, the failure of water pipes also resulted in the closure of dependent P3-P6, P5-R6, and R6-P7 segments, further dropping about 9.7 % of network efficiency. As a result of road closures, buildings nearby these segments experienced travel burden and physical accessibility lost to the nearest road segment (see Fig. 9(d)). The recovery of WDS was faster among these three networks, given that only one pipe completely breaks, and the repair time for damaged breaks and leaks is relatively faster than repairing extensively damaged electrical substations or bridges. Although WDS remained damaged for a shorter period than TN, WDS experienced a higher network efficiency loss compared to TN. This is because the TN network has more loops than WDS and a higher level of redundancy.

4.4.1.1. Hydraulic availability of WDS. The break in the WDS pipeline prevented water flow, whereas leaked pipelines experienced reductions in water flow volume. Pressure-dependent hydraulic simulation was performed using the Water Network Tool for Resilience (WNTR) to evaluate the hydraulic availability of WDS [60]. Damaged water pipelines were removed from the hydraulic model until they are repaired. Also, Pump Station PS3 was unable to provide water supply as a result of electricity outage until 7 days after the earthquake. As repair progresses, repaired pipelines are added back to the network for hydraulic simulation. Demand changes are also incorporated into the WDS hydraulic model during the restoration process. It is assumed that households will dislocate from buildings experiencing extensive or complete damage. For moderately damaged buildings, it was assumed for analysis purposes that households with an SV less than or equal to 0.2 will dislocate until their homes are repaired. SV score was generated using a scalable SV model developed by Enderami and Sutley [70] where a household with lower social vulnerability will have higher socioeconomic status and greater access to resources. Thus, approximately 46.1 %, 31.8 %, 8.5 %, 14.8 %, 15.4 %, 5.6 %, and 8.7 % of households dislocated immediately after the earthquake from zones Z1, Z2, Z3, Z4, Z5, Z6, and Z7, respectively. The ratio of dislocated households is

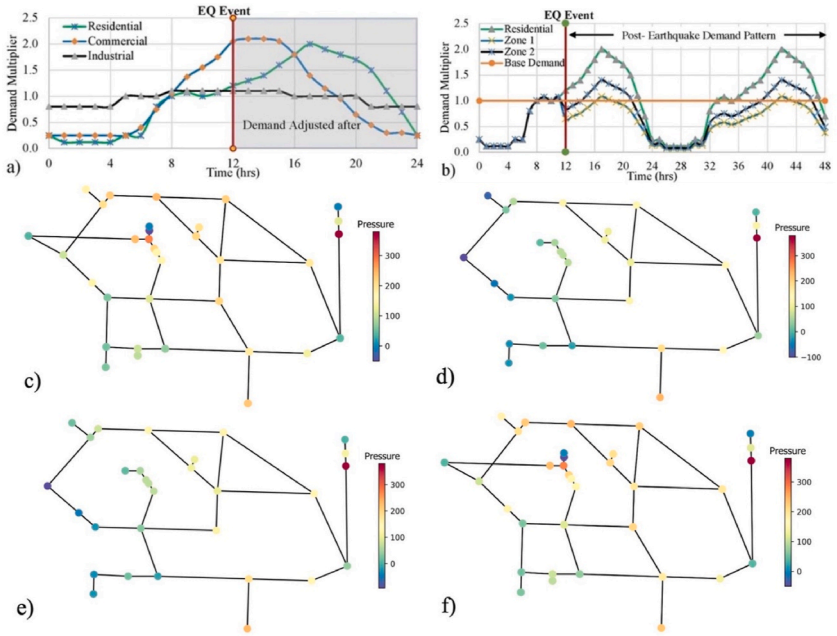

Fig. 12. Hydraulic performance of WDS: a) demand patterns (adapted from Ref. [20]), b) post-earthquake adjusted demand patterns for zones Z1 and Z2, c) pressure before earthquake, (d) at t = 0-hr (without dislocation), (e) at t = 0-hr (with demand changes), and (d) after repairing damaged pipelines.

correlated with building damage levels and household SV. Zone Z1 experienced a higher level of damage, as most buildings are comparatively more vulnerable (i.e., pre-code W2) than other wood buildings and experienced higher seismic intensities. Most households in zone Z1 have low SV and are high-income households, which contributes to a higher rate of dislocation from non-functional or partially functional households. Zones Z2 and Z3 are middle-income and low-density neighborhoods, but zone Z2 has a relatively lower level of SV and experienced a higher level of building damage than zone Z3. Therefore, a comparatively higher number of households are being dislocated from zone Z2. Zones Z4 and Z5 are middle-income housing with moderate levels of SV and experienced higher levels of damage. These zones have relatively lower levels of household dislocation compared to the higher damage levels. Zones Z6 and Z7 are low-income, high-density areas with mobile homes. However, zones Z6 and Z7 experienced the least amount of damage compared to other zones and therefore, have the lowest rate of household dislocation.

The regular fluctuation of demand for a particular node varies over time, and this variation was captured using demand patterns in hydraulic modeling of WDS [60]. The ratio of occupied housing units is used to update demand patterns. Fig. 12(a) shows daily demand patterns for residential, commercial, and industrial zones adapted herein from Guidotti et al. [20]. Assuming the earthquake hit at noon, the demand adjusted immediately after the occurrence of the earthquake until the community returned to its pre-earthquake state. Fig. 12(b) shows demand pattern adjustment for residential zones Z1 and Z2 for 36 h after the earthquake based on household dislocation. Demand drops to 53.4 % and 69.2 % immediately after the earthquake in these zones, eventually helping the damaged WDS to continue to meet the dynamic demand. While demand in residential zones were reduced due to household dislocation, it was assumed that service demands at critical facilities (i.e., hospitals) increased significantly due various reasons as applicable, including increased patient loads, extended stays, additional water to fight fires, sanitation needs, etc. Therefore, an adjustment factor of 2.5 was assumed based on expert knowledge to account for increased service demands at fire stations, hospitals, and other essential facilities. Characteristics of the WDS hydraulic model presented in Table 6 are obtained from IN-CORE [79].

Fig. 12(c)–(f) show pre-and post-earthquake hydraulic simulation results for the WDS. Fig. 12(c) and (d) show nodal pressure of WDS before and immediately after the earthquake, respectively. Seven damaged pipelines were removed from the hydraulic model, as shown in Fig. 12(d). The failure of water pipelines L01 and L24 disconnected Zone Z1 from the water reservoir. As a result of pipeline damages, pressure dropped significantly throughout the damaged WDS. For instance, zones Z1, Z9, Z4, and one fire station experienced partial water outages. However, the integration of demand changes due to household dislocation in residential zones and increased water demand at essential facilities alters the performance of the damaged WDS, as shown in Fig. 12(e). While water availability increases near residential zones, WDS cannot supply adequate water to the regional hospital. This can be visually determined by comparing Figs. 12(e) and 4(a). The performance of WDS returns to its normal state after repairing damaged pipelines as shown in Fig. 12(d). The incorporation of changes in water demand alters the performance of the WDS significantly during the repair process. As a result of significant pressure drops at demand nodes related to zones Z2, Z8, and Z10, these zones suffer from partial water outages. However, since a large portion of households dislocated from Z1 and Z2, the reduction in demand helps the WDS to satisfy revised demand even after sustaining physical damage.

4.4.2. Building functionality

Repair was simulated for all damaged buildings (except housing units whose households ended in stage 5 failure in the HHHR model). Building functionality was estimated by integrating physical performance with infrastructure inputs. Centerville suffered extensive building damage, as listed in Table 3. Water and power outages exacerbated the situation and dominated the functionality of buildings. Zones Z1, Z4, Z9, Z11, and regional hospitals suffered from electrical power outages. Zones Z2, Z8, Z10, and regional hospitals (located near Z1) suffered from partial water outages, and a large area of zone Z5 lost physical access to nearest roads due to damage in bridge B3 and nearby water pipe failures (see Figs. 9(d) and 14(a)). Residential Z3 and retail business Z9 also experience road accessibility burden due to the failure of nearby water pipe, and bridge B7. Fig. 13 shows various stages of post-earthquake functionality of buildings. Fig. 13(a) shows building functionality immediately after the earthquake, where approximately 20 % of

Table 6
Characteristics of water distribution systems.

Zone	Node ID	Elevation (m)	Base Demand (LPS)	Head(m)	Pattern
Z11	N14	510	35.7	735.97	Industrial
Z4	N11	580	71	970.77	Residential
GOVT	N08	535	57.4	971.16	Commercial
HS	N04	500	7.5	971.16	Commercial
Z1	N03	660	74.5	763.37	Residential
Z9	N10	590	71.8	971.42	Industrial
Z3	N06	550	11.6	736.42	Residential
Z10	N01	500	78.1	736.4	Industrial
Z9	N07	595	8.9	970.78	Commercial
FS	N21	555	7.9	970.72	Commercial
Hosp	N31	540	7.9	736.34	Commercial
Z7	N02	520	39.3	736.35	Residential
Z6	N05	550	65.4	736.32	Residential
Z8	N09	525	66.8	736.08	Commercial
Z5	N12	555	91	736.09	Residential
Z2	N13	605	97.3	737.77	Residential

Fig. 13. Functionality of buildings after: a) the earthquake, b) 3.02-days, c) 6.1-days, d) 7-days, e) 14-days, f) 75-days, g) 220-days, and h) 900-days.

buildings sustained extensive or complete damage, resulting in buildings being unsafe to occupy and non-functional. Failure of substations P8 and P6 resulted in an electrical outage in the entire Z1, part of Z4, and some heavy industry buildings in Zone Z11. Water pipes failure imposed partial water outage in zones Z9, Z5, and Z11. Further, the failure in the water pipe resulted in the closure of P5-R6, and R6-P7 road segments for pipeline repair, and bridge failures resulted in the closure of Robinson Street (R3-R4), and Linsey Street (R5-R6), leading to road accessibility losses in nearby buildings. Approximately 48 %, 9 %, and 43 % of buildings became non-functional, partially functional, and fully functional, respectively. At 3 days after the earthquake, the broken pipeline was repaired, and a few buildings at the edge of zone Z1 became functional. Although water service in zone Z1 is restored, buildings in Z1 remained non-functional due to electrical outage, as shown in Fig. 13(b). Just over six days are required to repair damaged components of WDS. As a result of collocated pipe repair, road segments P5-R6 and R6-P7 have been reopened. Therefore, functionality is fully restored in many buildings in zones Z5 and Z6, but power outages remain in Z1, Z4, Z9, and Z11, as shown in Fig. 13(c).

It took 7 days to repair sub-distribution P8, and another 7 days for repairing substation P6. After 7-days, functionality was restored in repaired and undamaged buildings in zones Z1, Z4, as shown in Fig. 13(d). Functionality of the regional hospital and high school were also affected due to electrical power outage in substation P8. The regional hospital suffered from partial water outages (about 30 % water shortage) due to increased water demand. Approximately 22 %, 3 %, and 75 % of buildings became non-functional, partially

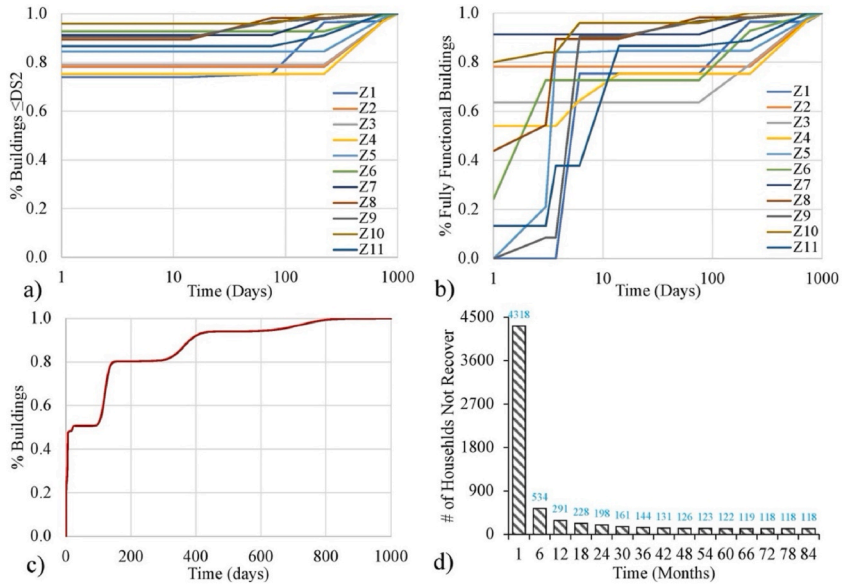

Fig. 14. Restoration process: (a) building damage repair by zone, (b) functionality restoration by zone, (c) overall damage repair, and (d) household recovery.

functional, and fully functional, respectively, after 7-days. Building functionality is significantly restored in zones Z4 and Z5 after restoring substation P6 after 14-days (see Fig. 13(e)). After 75-days, repairing bridge B3 restored the shortest path accessible to buildings in Z4 and Z5 (see Fig. 13(f)). Further, it took on average 120 days to repair extensively damaged RES2 buildings and more

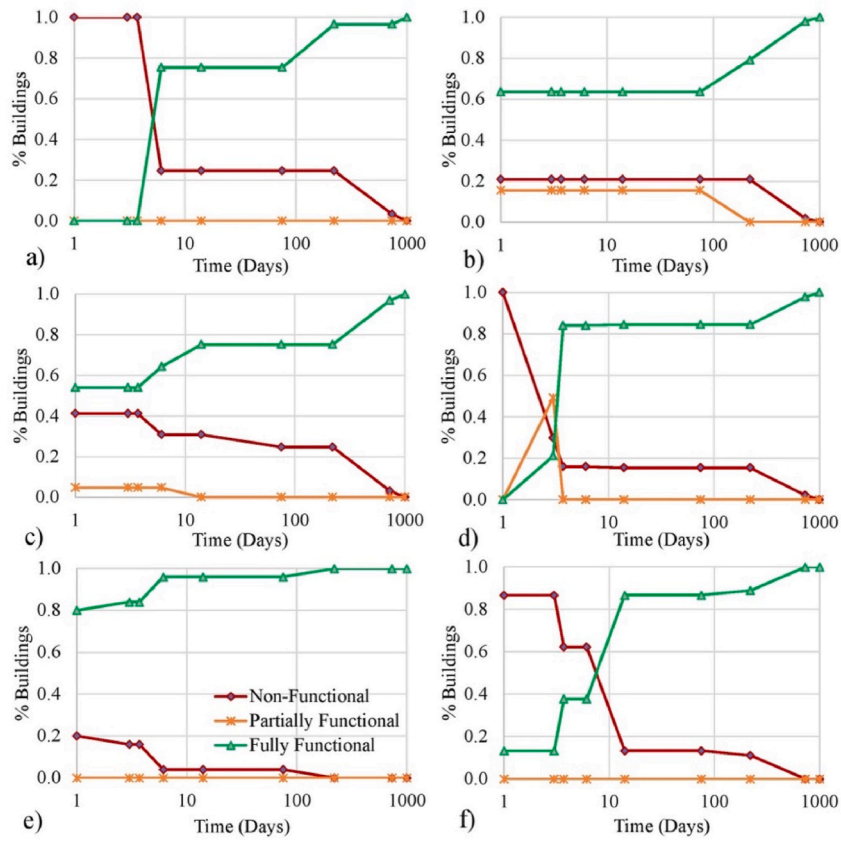

Fig. 15. Functionality of zone:(a) Z1, (b) Z3, (c) Z4, (d) Z5, (e) Z8 and (f) Z11.

time to repair other buildings experiencing damage ≥ DS3. After 220 days, bridge B7 is repaired resulting in partially functional buildings in Z6 becoming fully functional. At the same time, all RES2 that experienced ≤ DS3 become fully functional (see Fig. 13(g)). Fig. 13(h) shows that 99.5 % of buildings are fully recovered after 900 days of recovery.

Fig. 14(a) and (b) compare the damage repair and functionality restore of buildings. Residential building zones Z1-Z4 have the slowest repair trajectories, whereas industrial building zones (i.e., zones Z8, Z9, and Z11) have relatively quicker repair patterns due to a lower amount of building damages in industrial zones. This is also because the expected repair time for damaged industrial or commercial buildings is faster than the expected repair time for residential buildings. Buildings in mixed-use zones Z5-Z7 and Z10 repair faster than other residential zones but slower than industrial zones. Consideration of infrastructure service significantly alters the restoration process, particularly at the beginning of the functionality restoration (i.e., until 14 days) when infrastructure suffers outages. Fig. 14(c) shows the repair of all damaged buildings. An estimated 100, 125, and 900 days were required to repair approximately 50 %, 75 %, and 99 % of buildings, respectively. The HHHR model outcomes were integrated into the functionality restoration process. An estimated 124 households from mobile homes, 288 households from 48-dwellings multifamily buildings, and 4267 households from single-family homes are dislocated. Of these 4639 households, 1342 households' homes experience moderate damage but were predicted to dislocate due to their low SV (≤0.2). The remaining 3297 households were forced to dislocate due to extensive or complete damage to their home. The HHHR analysis was performed for the 4391 households residing in mobile homes and single-family homes but not for multifamily dwellings. Fig. 14(d) shows the number of households that did not achieve permanent housing during the 7-year post-earthquake recovery period. The HHHR model predicts that 88 % of households return to permanent housing after 6 months, where damage had not been fully repaired for 70 % of those households by this time. Buildings experienced damaged > DS2 typically require at least about 240 days to complete the repair process. Recovery was mostly completed for dislocated households in RES2 housing that sustained moderate damage. At the end of the recovery simulation, 118 households permanently failed to recover. Thus, 64, 40, and 14 households from Z4, Z5, and Z3, respectively, permanently became homeless, where the repair trajectory of their pre-disaster homes then becomes beyond the scope of the present analysis.

Semi-log Fig. 15 plots the functionality restoration of the six zones that sustain relatively higher functionality losses than the other zones. This process accounted for coupled outcomes of the damage repair and the HHHR model. Fig. 15(a) shows that about 75 % of buildings became fully functional after electricity is restored in zone Z1. Functionality restoration of the rest of the buildings (25 %) in this zone is dominated by physical repair. Buildings in this zone did not experience physical accessibility loss to roads. About 20 %, 40 %, and 100 % of buildings in zones Z3, Z4, and Z5, respectively, became non-functional, as shown in Fig. 15(b)–15(d). About 15 % and 5 % of buildings experience partial functionality loss in zones Z3 and Z4, respectively, due to road accessibility loss. Zone 5 initially suffers from water outage, and all buildings became non-functional. After the water pipeline is repaired at 3.7 days post-earthquake, 20 % and 50 % of buildings became fully functional and partially functional, respectively. Fig. 15(e) and (f) show the functionality restoration trajectory of retail/business zone Z8 and heavy industry zone Z11, respectively. Z8 suffered an initial 20 % of functionality loss, and Z11 experienced 85 % of initial functionality loss before restoring. As an overall trend, after water and power are restored after 14 days, functionality restoration is dominated by the estimated physical repair of buildings.

5. Conclusions

This paper proposes a functionality analysis framework that incorporates multiple interdependent infrastructure systems with buildings with an updated performance metrics into community disaster resilience analysis. The key contributions of the framework include the following.

- This framework accounts for coupled interaction among the buildings and infrastructure systems, and household-level housing recovery to estimate the functionality of buildings at the community level. The framework incorporates the road network physical accessibility to buildings in the functionality evaluation of buildings.
- The current approach addresses the changes in demands on WDS due to household dislocation and return, and increased service demand on essential facilities throughout the recovery and restoration process following an earthquake, which is often ignored in past studies.
- The cascading impacts of water pipeline failure on TN are modelled through geographic dependency analysis. GIS buffer analysis is performed to identify the physically collocated water and road segments. Input-output interdependency is modelled between WDS and EPN.
- The performance of the buildings and infrastructure systems are determined separately. Then, the interaction between buildings and infrastructure systems is modelled through input-output physical linkage. Service area of infrastructure systems is approximated using Voronoi polygons. Network theory is applied to evaluate the performance of infrastructure nodes and dependent building zones. The links between physical and social systems are established by modeling household dislocation and re-occupancy considering the household's social vulnerability and the extent of home damage.

Recent disasters resulted in functionality losses and brought enormous consequences to the community despite the buildings remaining physically operable after the disaster. The proposed functionality analysis can provide useful insights for decision-making in mitigating the impact of natural disasters. This model can account for the effect of utility serviceability and reflect real-world scenarios in the aftermath of a disaster. Although the current approach is explained for post-earthquake functionality and resilience analysis, the proposed resilience analysis framework can be applied to a general class of interconnected infrastructure systems and buildings and any hazard type that causes physical damage. The case study findings reveal that the consideration of utility availability and road

network physical access to buildings significantly alters the functionality of building clusters. A large part of the building portfolio lost functionality, even though they were physically operable immediately after the earthquake. The restoration process shows that the recovery of buildings was slower than the recovery of infrastructure systems, which dominates the recovery process. Approximately 75 %, 64 %, 30 %, and 60 % of buildings lost functionality in zones Z1, Z4, Z5, and Z11 during infrastructure serviceability restoration until 14 days after the earthquake. WDS had the shortest recovery time. In comparison to WN and EPN, TN had a longer recovery time. The cascading effect of water pipeline failure on TN significantly alters the network efficiency of TN. Collocated water pipeline failures resulted in nearby road segment closures, leading to an additional 9.7 % drop in network efficiency for TN. Changes in demand and infrastructure interdependency also significantly influence the functionality of the community.

The framework can be used to analyze existing systems for vulnerabilities, as well as to explore potential mitigation and adaptation strategies, such as increasing redundancy and/or hardening one or more of the infrastructure systems or strategically deploying repair and recovery resources to reduce specific resilience metrics such as recovery times for infrastructure systems, number of dislocated households, or number of households becoming homeless. There exist a few limitations that should be considered in future study. The recovery assessment assumed that each network and community have sufficient recovery resources, which will vary significantly across communities and hazard events. Correlation of seismic intensities and damages was not accounted for while estimating seismic intensities and physical damages. Physical accessibility loss to nearest road segment may further delay in engineering inspection and repair process, which was ignored. Building repair process adopted from FEMA [57] accounted for associated inspection, permission delay, and repair time. However, the restoration of damaged infrastructure components depends on many factors, including available recovery resources, repair crew availability, accessibility, weather, equipment availability, travel time to the damage location, etc., which were not accounted for in the recovery estimation, and recovery process assumed only one repair could be performed at a time for each infrastructure system. The HHHR model is applied only to single-family households, as the recovery of multi-family housing involves different social vulnerabilities and recovery mechanisms. Future studies may be expanded to include a multi-family housing recovery and a detailed household dislocation model that reflects realistic changes in demand on infrastructure systems. The proposed framework is applied to a virtual testbed, which needs further application to real network. The application of current framework is computationally intensive, particularly for a large community with hundreds of infrastructure components. Therefore, we executed an illustrative example by developing a Python script following the algorithm provided in Fig. 4, which is time-efficient (e.g., one simulation took 40 min on a personal computer with 8 GB RAM and an Apple M1 chip with an 8-core CPU) and requires less computational cost.

CRediT authorship contribution statement

Ram Krishna Mazumder: Writing – original draft, Conceptualization, Methodology formulation, Analysis, Data curation. **Elaina J. Sutley:** Writing – review & editing, Supervision, Investigation, Funding acquisition.

Declaration of competing interest

The authors declare that they have no known competing financial interests or personal relationships that could have appeared to influence the work reported in this paper.

Acknowledgement

This work was partially supported by the National Science Foundation under Grant No. CMMI 1847373. This work was also partially supported by the NIST-funded Center of Excellence for Risk-Based Community Resilience Planning. Funding for this study was provided as part of the Center's cooperative agreement between the U.S. NIST and Colorado State University (Grant Number 70NANB15H044). The views expressed are those of the author(s), and do not necessarily reflect the views of the National Science Foundation, NIST, or the U.S. Department of Commerce.

Appendix

Table A1
Fragility parameters for infrastructure components (Adapted from FEMA [57] and Nielson and DesRoches [58])

Component Type	PGA (g)							
	Slight		Moderate		Extensive		Complete	
	λ	ζ	λ	ζ	λ	ζ	λ	ζ
Low-Volt Distribution Substation	0.15	0.70	0.29	0.55	0.45	0.45	0.90	0.45
Medium-Volt Main Grid Substation	0.15	0.60	0.25	0.50	0.35	0.40	0.70	0.40
High-Volt Transmission Substation	0.11	0.50	0.15	0.45	0.20	0.35	0.47	0.40
Steel Tank	0.30	0.60	0.70	0.60	1.25	0.65	1.60	0.60

(*continued on next page*)

Table A1 (*continued*)

Component Type	PGA (g)							
	Slight		Moderate		Extensive		Complete	
	λ	ζ	λ	ζ	λ	ζ	λ	ζ
Concrete Tank	0.25	0.55	0.52	0.70	0.95	0.60	1.64	0.70
MSC Concrete	0.15	0.70	0.52	0.70	0.75	0.70	1.03	0.70
MSSS Concrete	0.20	0.65	0.57	0.65	0.83	0.65	1.17	0.65

Note: λ: median, ζ: log-standard deviation.

Table A2
Fragility parameters for building structural archetypes [57].

Building Type	Design Code	PGA (g)							
		Slight		Moderate		Extensive		Complete	
		λ	ζ	λ	ζ	λ	ζ	λ	ζ
W1	pre-code W2	0.12	0.64	0.19	0.64	0.37	0.64	0.60	0.64
W2	low-code W1	0.20	0.64	0.34	0.64	0.61	0.64	0.95	0.64
W3	moderate-code W1	0.24	0.64	0.43	0.64	0.91	0.64	1.34	0.64
W4	pre-code W1	0.18	0.64	0.29	0.64	0.51	0.64	0.77	0.64
W5	low-code W2	0.14	0.64	0.23	0.64	0.48	0.64	0.75	0.64
W6	low-code MH	0.11	0.64	0.18	0.64	0.31	0.64	0.60	0.64
S1	low-code S2L	0.13	0.64	0.17	0.64	0.30	0.64	0.50	0.64
RC1	low-code C1L	0.12	0.64	0.15	0.64	0.27	0.64	0.45	0.64
RM1	pre-code RM1L	0.13	0.64	0.16	0.64	0.24	0.64	0.43	0.64
S2	low-code S3	0.10	0.64	0.13	0.64	0.20	0.64	0.38	0.64
S3	pre-code S2L	0.11	0.64	0.14	0.64	0.23	0.64	0.39	0.64
S4	moderate-code S2L	0.20	0.64	0.26	0.64	0.46	0.64	0.84	0.64
RC2	low-code C1M	0.12	0.64	0.17	0.64	0.32	0.64	0.54	0.64
RM2	low-code RM1L	0.16	0.64	0.20	0.64	0.29	0.64	0.54	0.64
RC3	moderate-code C1L	0.16	0.64	0.23	0.64	0.41	0.64	0.77	0.64
RM3	moderate-code RM1L	0.22	0.64	0.30	0.64	0.50	0.64	0.85	0.64

Note: λ: median, ζ: log-standard deviation.

Data availability

Data will be made available on request.

References

[1] L.F. Gay, S.K. Sinha, Novel resilience assessment methodology for water distribution systems, in: Pipelines 2012: Innovations in Design, Construction, Operations, and Maintenance, 2012, pp. 61–69, doing more with less.
[2] G.P. Cimellaro, A. Tinebra, C. Renschler, M. Fragiadakis, New resilience index for urban water distribution networks, J. Struct. Eng. 142 (8) (2016) C4015014.
[3] K. Diao, C. Sweetapple, R. Farmani, G. Fu, S. Ward, D. Butler, Global resilience analysis of water distribution systems, Water Res. 106 (2016) 383–393.
[4] R.K. Mazumder, A.M. Salman, Y. Li, X. Yu, Seismic functionality and resilience analysis of water distribution systems, J. Pipeline Syst. Eng. Pract. 11 (1) (2020) 04019045.
[5] M. Ouyang, L. Dueñas-Osorio, X. Min, A three-stage resilience analysis framework for urban infrastructure systems, Struct. Saf. 36 (2012) 23–31.
[6] M. Ouyang, L. Duenas-Osorio, Multi-dimensional hurricane resilience assessment of electric power systems, Struct. Saf. 48 (2014) 15–24.
[7] M. Panteli, C. Pickering, S. Wilkinson, R. Dawson, P. Mancarella, Power system resilience to extreme weather: fragility modeling, probabilistic impact assessment, and adaptation measures, IEEE Trans. Power Syst. 32 (5) (2016) 3747–3757.
[8] A. Alipour, B. Shafei, Seismic resilience of transportation networks with deteriorating components, J. Struct. Eng. 142 (8) (2016) C4015015.
[9] W. Zhang, N. Wang, C. Nicholson, Resilience-based post-disaster recovery strategies for road-bridge networks, Structure and Infrastructure Engineering 13 (11) (2017) 1404–1413.
[10] I. Kilanitis, A. Sextos, Integrated seismic risk and resilience assessment of roadway networks in earthquake prone areas, Bull. Earthq. Eng. 17 (1) (2019) 181–210.
[11] Y. Gu, X. Fu, Z. Liu, X. Xu, A. Chen, Performance of transportation network under perturbations: reliability, vulnerability, and resilience, Transport. Res. E Logist. Transport. Rev. 133 (2020) 101809.
[12] P. Juan-Garcia, D. Butler, J. Comas, G. Darch, C. Sweetapple, A. Thornton, L. Corominas, Resilience theory incorporated into urban wastewater systems management. State of the art, Water Res. 115 (2017) 149–161.
[13] C. Sweetapple, M. Astaraie-Imani, D. Butler, Design and operation of urban wastewater systems considering reliability, risk and resilience, Water Res. 147 (2018) 1–12.
[14] C. He, C. Dai, L. Wu, T. Liu, Robust network hardening strategy for enhancing resilience of integrated electricity and natural gas distribution systems against natural disasters, IEEE Trans. Power Syst. 33 (5) (2018) 5787–5798.
[15] G.P. Cimellaro, O. Villa, M. Bruneau, Resilience-based design of natural gas distribution networks, J. Infrastruct. Syst. 21 (1) (2015) 05014005.
[16] M.V. Comber, C.D. Poland, Disaster resilience and sustainable design: Quantifying the benefits of a holistic design approach, in: Structures Congress 2013: Bridging Your Passion with Your Profession, 2013, pp. 2717–2728.
[17] H.V. Burton, G. Deierlein, D. Lallemant, T. Lin, Framework for incorporating probabilistic building performance in the assessment of community seismic resilience, J. Struct. Eng. 142 (8) (2016) C4015007.

[18] P. Lin, N. Wang, Building portfolio fragility functions to support scalable community resilience assessment, Sustainable and Resilient Infrastructure 1 (3–4) (2016) 108–122.
[19] I. Hernandez-Fajardo, L. Dueñas-Osorio, Probabilistic study of cascading failures in complex interdependent lifeline systems, Reliab. Eng. Syst. Saf. 111 (2013) 260–272.
[20] R. Guidotti, H. Chmielewski, V. Unnikrishnan, P. Gardoni, T. McAllister, J. van de Lindt, Modeling the resilience of critical infrastructure: the role of network dependencies, Sustainable and resilient infrastructure 1 (3–4) (2016) 153–168.
[21] S.Y. Lin, S. El-Tawil, Time-dependent resilience assessment of seismic damage and restoration of interdependent lifeline systems, J. Infrastruct. Syst. 26 (1) (2019) 04019040.
[22] S.B. Miles, S.E. Chang, ResilUS: a community-based disaster resilience model, Cartography and Geographic Information Science 38 (1) (2011) 36–51.
[23] W. Zhang, P. Lin, N. Wang, C. Nicholson, X. Xue, Probabilistic prediction of postdisaster functionality loss of community building portfolios considering utility disruptions, J. Struct. Eng. 144 (4) (2018) 04018015.
[24] H. Masoomi, H. Burton, A. Tomar, A. Mosleh, Simulation-based assessment of postearthquake functionality of buildings with disruptions to cross-dependent utility networks, J. Struct. Eng. 146 (5) (2020) 04020070.
[25] V. Terzic, P.K. Villanueva, D. Saldana, D.Y. Yoo, Framework for modelling post-earthquake functional recovery of buildings, Eng. Struct. 246 (2021) 113074.
[26] D.T. Cook, A.B. Liel, C.B. Haselton, M. Koliou, A framework for operationalizing the assessment of post-earthquake functional recovery of buildings, Earthq. Spectra 38 (3) (2022) 1972–2007.
[27] C. Molina Hutt, A.M. Hulsey, P. Kakoty, G.G. Deierlein, A. Eksir Monfared, Y. Wen-Yi, J.D. Hooper, Toward functional recovery performance in the seismic design of modern tall buildings, Earthq. Spectra 38 (1) (2022) 283–309.
[28] R.K. Mazumder, S.A. Enderami, E.J. Sutley, A novel framework to study community-level social and physical impacts of hurricane-induced winds through synthetic scenario analysis, Frontiers in Built Environment 9 (2023) 1005264.
[29] M. Aghababaei, M. Koliou, Community resilience assessment via agent-based modeling approach, Comput. Aided Civ. Infrastruct. Eng. 38 (7) (2023) 920–939.
[30] N. Blagojević, V. Terzić, B. Stojadinović, F-RecN+ iRe-CoDeS: computational framework for regional recovery simulation using advanced building recovery models, Eng. Struct. 288 (2023) 116156.
[31] E.A. Opabola, C. Galasso, A probabilistic framework for post-disaster recovery modeling of buildings and electric power networks in developing countries, Reliab. Eng. Syst. Saf. 242 (2024) 109679.
[32] N. Coleman, A. Esmalian, A. Mostafavi, Equitable resilience in infrastructure systems: empirical assessment of disparities in hardship experiences of vulnerable populations during service disruptions, Nat. Hazards Rev. 21 (4) (2020) 04020034.
[33] D. Mitsova, A.M. Esnard, A. Sapat, A. Lamadrid, M. Escaleras, C. Velarde-Perez, Effects of infrastructure service disruptions following hurricane Irma: Multilevel analysis of postdisaster recovery outcomes, Nat. Hazards Rev. 22 (1) (2021) 04020055.
[34] C.A. Davis, Understanding functionality and operability for infrastructure system resilience, Nat. Hazards Rev. 22 (1) (2021) 06020005.
[35] S.A. Enderami, E.J. Sutley, S.L. Hofmeyer, Defining organizational functionality for evaluation of post-disaster community resilience, Sustainable and Resilient Infrastructure (2021) 1–18.
[36] M. Watson, Y. Xiao, J. Helgeson, M. Dillard, Importance of households in business disaster recovery, Nat. Hazards Rev. 21 (4) (2020) 05020008.
[37] M. Aghababaei, M. Koliou, An agent-based modeling approach for community resilience assessment accounting for system interdependencies: application on education system, Eng. Struct. 255 (2022) 113889.
[38] M.W. Mieler, J. Mitrani-Reiser, Review of the state of the art in assessing earthquake-induced loss of functionality in buildings, J. Struct. Eng. 144 (3) (2018) 04017218.
[39] J.B. Nevill, F.T. Lombardo, Structural functionality scale for light-Framed wood buildings with indicators for Windstorm damage, J. Struct. Eng. 146 (4) (2020) 04020033.
[40] P. Lin, N. Wang, Stochastic post-disaster functionality recovery of community building portfolios II: application, Struct. Saf. 69 (2017) 106–117.
[41] E.J. Sutley, S. Hamideh, An interdisciplinary system dynamics model for post-disaster housing recovery, Sustainable and Resilient Infrastructure 3 (3) (2018) 109–127.
[42] I. Almufti, M. Willford, REDiTM Rating System: Resiliencebased Earthquake Design Initiative for the Next Generation of Buildings, Arup Co, London, 2013.
[43] N. Mohammadgholibeyki, M.J. Echeverria, A. Safiey, D. Cook, M. Koliou, A.B. Liel, Assessing the feasibility of achieving functional recovery goals through seismic retrofit of existing reinforced concrete buildings, Earthq. Spectra 39 (4) (2023) 2123–2151.
[44] N. Mohammadgholibeyki, M. Koliou, A.B. Liel, Assessing building's post-earthquake functional recovery accounting for utility system disruption, Resilient Cities and Structures 2 (3) (2023) 53–73.
[45] J. Mitrani-Reiser, M. Mahoney, W.T. Holmes, J.C. De La Llera, R. Bissell, T. Kirsch, A functional loss assessment of a hospital system in the Bío-Bío province, Earthq. Spectra 28 (1_suppl1) (2012) 473–502.
[46] H. Masoomi, J.W. van de Lindt, Restoration and functionality assessment of a community subjected to tornado hazard, Structure and Infrastructure Engineering 14 (3) (2018) 275–291.
[47] M. Ghosn, L. Dueñas-Osorio, D.M. Frangopol, T.P. McAllister, P. Bocchini, L. Manuel, G. Tsiatas, Performance indicators for structural systems and infrastructure networks, J. Struct. Eng. 142 (9) (2016) F4016003.
[48] S.M. Rinaldi, J.P. Peerenboom, T.K. Kelly, Identifying, understanding, and analyzing critical infrastructure interdependencies, IEEE control systems magazine 21 (6) (2001) 11–25.
[49] M. Ouyang, Review on modeling and simulation of interdependent critical infrastructure systems, Reliab. Eng. Syst. Saf. 121 (2014) 43–60.
[50] R.K. Mazumder, A.M. Salman, Y. Li, X. Yu, Asset management decision support model for water distribution systems: impact of water pipe failure on road and water networks, J. Water Resour. Plann. Manag. 147 (5) (2021) 04021022.
[51] R. Ceskavich, M. Sasani, Methodology for evaluating community resilience, Nat. Hazards Rev. 19 (1) (2018) 04017021.
[52] M.R. Ameri, J.W. van de Lindt, Seismic performance and recovery modeling of natural gas networks at the community level using building demand, J. Perform. Constr. Facil. 33 (4) (2019) 04019043.
[53] N. Mohammadgholibeyki, M. Koliou, A.B. Liel, A simple network-based probabilistic method for estimating recovery of lifeline services to buildings after an earthquake, Structure and Infrastructure Engineering (2023) 1–17.
[54] N. Rosenheim, R. Guidotti, P. Gardoni, W.G. Peacock, Integration of detailed household and housing unit characteristic data with critical infrastructure for post-hazard resilience modeling, Sustainable and Resilient Infrastructure (2019) 1–17.
[55] R. Guidotti, P. Gardoni, N. Rosenheim, Integration of physical infrastructure and social systems in communities' reliability and resilience analysis, Reliab. Eng. Syst. Saf. 185 (2019) 476–492.
[56] Y.S. Lin, Development of Algorithms to Estimate Post-disaster Population Dislocation—A Research-Based Approach, Texas A&M University, 2009.
[57] FEMA, Multi-hazard Loss Estimation Methodology Earthquake Model HAZUS-MH 2.1 Technical Manual, FEMA, Washington, DC, 2012.
[58] B.G. Nielson, R. DesRoches, Analytical seismic fragility curves for typical bridges in the central and southeastern United States, Earthq. Spectra 23 (3) (2007) 615–633.
[59] ALA (American Lifelines Alliance), Seismic Fragility Formulation for Water Systems, ASCE, Reston, VA, 2001.
[60] K.A. Klise, M. Bynum, D. Moriarty, R. Murray, A software framework for assessing the resilience of drinking water systems to disasters with an example earthquake case study, Environ. Model. Software 95 (2017) 420–431.
[61] R.K. Mazumder, X. Fan, A.M. Salman, Y. Li, X. Yu, Framework for seismic damage and renewal cost analysis of buried water pipelines, J. Pipeline Syst. Eng. Pract. 11 (4) (2020) 04020038.
[62] E.J. Sutley, S. Hamideh, Postdisaster housing stages: a Markov chain approach to model sequences and duration based on social vulnerability, Risk Anal. 40 (12) (2020) 2675–2695.
[63] P. Lin, N. Wang, Stochastic post-disaster functionality recovery of community building portfolios I: modeling, Struct. Saf. 69 (2017) 96–105.

[64] M. Shinozuka, X. Dong, T.C. Chen, X. Jin, Seismic performance of electric transmission network under component failures, Earthquake engineering & structural dynamics 36 (2) (2007) 227–244.
[65] R. Albert, I. Albert, G.L. Nakarado, Structural vulnerability of the North American power grid, Physical review E 69 (2) (2004) 025103.
[66] F. Hu, C.H. Yeung, S. Yang, W. Wang, A. Zeng, Recovery of infrastructure networks after localised attacks, Sci. Rep. 6 (1) (2016) 1–10.
[67] V. Latora, M. Marchiori, Efficient behavior of small-world networks, Phys. Rev. Lett. 87 (19) (2001) 198701.
[68] S.S. Ozger, L.W. Mays, A Semi-pressure-driven Approach to Reliability Assessment of Water Distribution Networks, Arizona State University, 2003 (Doctoral dissertation,.
[69] J.M. Wagner, U. Shamir, D.H. Marks, Water distribution reliability: simulation methods, J. Water Resour. Plann. Manag. 114 (3) (1988) 276–294.
[70] S.A. Enderami, E. Sutley, Social vulnerability score: a scalable index for representing social vulnerability in virtual community resilience testbeds, Nat. Hazards (2024), https://doi.org/10.1007/s11069-024-06499-z, 2024.
[71] A. Bosisio, A. Berizzi, M. Merlo, A. Morotti, G. Iannarelli, A GIS-based approach for primary substations siting and timing based on Voronoi Diagram and Particle Swarm Optimization method, Appl. Sci. 12 (12) (2022) 6008.
[72] A. Suvizi, A. Farghadan, M.S. Zamani, A parallel computing architecture based on cellular automata for hydraulic analysis of water distribution networks, J. Parallel Distr. Comput. 178 (2023) 11–28.
[73] O. Pala, D. Wilson, R. Bent, S. Linger, J. Arnold, Accuracy of service area estimation methods used for critical infrastructure recovery, in: Critical Infrastructure Protection VIII: 8th IFIP WG 11.10 International Conference, ICCIP 2014, Arlington, VA, USA, March 17-19, 2014, Revised Selected Papers 8, Springer Berlin Heidelberg, 2014, pp. 173–191.
[74] K.A. Porter, Damage and restoration of water supply systems in an earthquake sequence. Structural Engineering and Structural Mechanics Program, Department of Civil Environmental and Architectural Engineering, University of Colorado, 2016, p. 16, 02.
[75] B.R. Ellingwood, H. Cutler, P. Gardoni, W.G. Peacock, J.W. van de Lindt, N. Wang, The centerville virtual community: a fully integrated decision model of interacting physical and social infrastructure systems, Sustainable and Resilient Infrastructure 1 (3–4) (2016) 95–107.
[76] K. Kawashima, K. Aizawa, K. Takahashi, Attenuation of peak ground motion and absolute acceleration response spectra, in: Proceedings of the 8th World Conference on Earthquake engineering. San Francisco, California, USA, 1984, pp. 21–28. July.
[77] Y.X. Yu, C.Y. Jin, Empirical peak ground velocity attenuation relations based on digital broadband records, in: 14th World Conference on Earthquake Engineering, 2008. October 12-17, 2008, Beijing, China.
[78] A. Hagberg, P. Swart, D. S Chult, Exploring Network Structure, Dynamics, and Function Using NetworkX (No. LA-UR-08-05495; LA-UR-08-5495), Los Alamos National Lab.(LANL), Los Alamos, NM (United States), 2008.
[79] IN-CORE, The Interdependent Networked Community Resilience Modeling Environment (IN-CORE), 2021. http://resilience.colostate.edu/in-core. v.4.14.0.